Ph.D. Dissertation of

The synergistic effect of disulfiram with cisplatin in atypical teratoid/rhabdoid tumors (AT/RT)

비정형기형모양/횡문근육모양종양에서

다이설피람과 시스플라틴 병용치료의 상승효과

August 2019

Graduate School of Medicine

Seoul National University

Interdisciplinary Program in Stem Cell Biology

Anshika Jangra

The synergistic effect of disulfiram with cisplatin in atypical teratoid/rhabdoid tumors (AT/RT)

Kim Seung-Ki

A thesis submitted in partial fulfillment of the requirements for the degree of Doctor in Philosophy in Science to the faculty of Interdisciplinary Program in Stem Cell Biology

August 2019

Graduate School of Medicine

Seoul National University

By

Anshika Jangra

Doctoral Committee

Professor Kwon Wook Joo Chairman

Professor Seung-ki Kim Vice Chairman

Professor Jong Hee Chae

Professor Chul-Kee Park

Professor Ho Jun Seol

Abstract

Atypical teratoid/rhabdoid tumor (AT/RT) is the most malignant tumor of the central nervous system that generally occurs in children under three years of age. There is no effective chemotherapy to treat most AT/RT patients. Brain tumors have a small subpopulation of cells called cancer stem cells that do not respond to or are resistant to conventional anticancer drugs. In our previous studies, we observed the high expression of aldehyde dehydrogenase (ALDH), a stem cell marker in AT/RT cells. Based on this, we confirmed the anticancer effect of disulfiram, which is an ALDH inhibitor. Herein, we investigated the drug interaction between disulfiram and cisplatin against AT/RT cells *in vitro* and *in vivo.*

Patient-derived primary cultured cells (SNUH.AT/RT09 and SNUH.AT/RT11) and established cell lines (BT12 and BT16) were utilized for *in vitro* experiments. The combination effects of disulfiram with cisplatin was confirmed by cell viability, followed by the confirmation of drug interaction via isobologram. Further experiments include flow cytometry, ELISA, and immunofluorescence analysis. The mechanism of action was identified by western blot analysis. Tumor volumes and survival rates were analyzed via bioluminescence live imaging in an AT/RT orthotopic xenograft mouse model to verify *in vivo* therapeutic effects.

Our results demonstrate the anti-cancer effects with the combination of disulfiram and cisplatin in both *in vitro* and *in vivo*. The drug combination significantly inhibited the cell viability and showed synergism, confirmed by isobologram analysis and

also reduced ALDH enzyme activity of all AT/RT cells. The combination of disulfiram and cisplatin has shown to modulate pDNA-PKcs, γH2Ax, and ATF3 protein expression to activate PARP and thus induce apoptosis much more effectively. Importantly, the combination of disulfiram with cisplatin resulted in decreased tumor volume as indicated via IHC staining and increased long term survival rate in AT/RT animal models.

Our study suggests that disulfiram and cisplatin combination has a synergistic effect, which affects ATF3 within the cells leading to cellular apoptosis via cleaved PARP mechanism. This combination can be used as a novel treatment strategy for AT/RT, which is difficult to treat with conventional chemotherapy.

Keyword: Atypical teratoid/rhabdoid tumor, Aldehyde dehydrogenase, Disulfiram, Cisplatin, Activating transcription factor 3

Student Number: 2015-30725

Table of Contents

List of Abbreviations v

List of Tables vii

List of Figures viii

Introduction 1

Materials and methods 9

1.1 Cell cultures 9

1.2 Cell viability analysis 11

1.3 Fluorescence-activated cell sorting (FACS) 11

1.4 Enzyme-linked immunosorbent assay (ELISA) 12

1.5 Western blot 12

1.6 Orthotopic AT/RT xenograft mouse model 13

1.7 Drug treatment *in vivo* 13

1.8 *In vivo* live imaging and survival analysis 14

1.9 Histological analysis 14

1.10 Immunofluorescence staining 15

Results 16

2.1 Synergistic effect of disulfiram and cisplatin in combination treatment 16

2.2 Decreased ALDH enzyme activity by combination treatment 26

2.3 Regulation of ATF3 leading to apoptosis in AT/RT cells 29

2.4 Increased survival in long term *in vivo* 33

2.5 Reduction in tumor volume and immunofluorescence staining 39

Discussion 42

References 51

Abstract in Korean 69

List of Abbreviations

ALDH, Aldehyde dehydrogenase

AT/RT, Atypical teratoid rhabdoid tumor

BTICs, Brain tumor-initiating cells

BTSCs, Brain tumor stem cells

BTICs, Brain tumor-initiating cells

CIS, Cisplatin

CNS, Central nervous system

CSCs, Cancer stem cells

DEAB, Diethylaminobezaldehyde

DMEM, Dulbecco's modified Eagle's medium

DMSO, Dimethyl sulfoxide

ELISA, Enzyme-linked immune sorbent assay

FACS, Fluorescence-activated cell sorting

FDA, Food and Drug Association

FITC, Fluorescein isothiocyanate

H&E, Hematoxylin and eosin

IACUC, Institutional Animal Care and Use Committee

IC_{50}, Inhibitory concentration at 50%

IRB, Institutional review board

JNK, c-Jun N-terminal protein kinase

MAPK, Microtubule-associated protein kinase

MYC, Myelocytomatosis

NADH, Nicotinamide adenine dinucleotide-Hydrogen (reduced)

NSCs, Neural stem cells

OCT, Optimal Cutting temperature compound

PBS, Phosphate buffer saline

PNET, Primitive neuroectodermal tumor

RIPA, Radioimmunoprecipitation assay

RT, Radiation therapy

SHH, Sonic Hedgehog

SMARCB1, SWI/SNF-related matrix-associated actin-dependent regulator of chromatin subfamily B member 1

SWI/SNF, SWItch/Sucrose Non-Fermentable

TYR, Tyrosin

WHO, World Health Organization

List of Tables

Table 1 – Patient information 10

Table 2 – Half-Maximal Inhibitory Concentration ($IC_{50)}$, μM 19

Table 3 – CI value calculation for cisplatin in combination with disulfiram 22

Table 4 – CI value calculation for etoposide in combination with disulfiram 23

Table 5 – Quantification of tumor growth by bioluminescence image (BLI) 36

Table 6 – p-value comparison analysis of region of interest (ROI) values 37

List of Figures

Figure 1– Cell viability of disulfiram with conventional drugs 18

Figure 2– Cell viability of disulfiram and cisplatin confirming the IC_{50} 20

Figure 3– Cell viability of disulfiram and etoposide confirming the IC_{50} 21

Figure 4– Drug treatment at different time intervals 24

Figure 5 – Synergistic effect of disulfiram and cisplatin on primary cultured cells and established cell lines 25

Figure 6– ALDH positive cell population in primary cultured cells and established cell lines 27

Figure 7 – ALDH enzyme activity in primary cultured cells and established cell lines 28

Figure 8 – Predicted mechanism of ATF3, MAPK and ALDH1A1 pathway affected by disulfiram and cisplatin working in synergism 30

Figure 9 – Western blot analysis in AT/RT cells 31

Figure 10– Quantification of western blot proteins 32

Figure 11– *In vivo* schematic diagram for drug treatment 34

Figure 12– Long–term treatment of disulfiram and cisplatin combination therapy 35

Figure 13– Comparison of body weight in BT16 effluc mice model 38

Figure 14– *In vivo* Immunofluorescence analysis of drug combination 40

Figure 15– Quantification of tumor volume and immunofluorescence data *in vivo* 41

Introduction

Atypical teratoid/rhabdoid tumor was described as a distinct entity in 1987. Earlier they were misdiagnosed as medulloblastoma and rhabdoid tumor (D.-T. Ho, Hsu, Wong, Ting, & Chiang, 2000). By 1995, they were regarded as a newly defined aggressive tumor that affects the brain and spinal cord and dominantly affected infants and young children. AT/RT currently constitutes one of three primary embryonal tumors in 2007 World Health Organization classification of Central nervous system (CNS) tumors and is accorded grade IV by WHO due to its malignant nature (Louis et al., 2007). About 17% of all the pediatric cancers involve the CNS, making these cancers the most common childhood solid tumor. After leukemia, pediatric brain tumor is the second leading cause of childhood death (Gessi, Giangaspero, & Pietsch, 2003). Recent trends also suggest that the rate of overall CNS tumor diagnosis is on the rise by about 2.7% each year. Since the diagnostic techniques use genetic markers, the proportion of AT/RT diagnosis is expected to also increase per year. Recent studies that use multimodal therapeutic techniques have shown improvement in survival rate. In 2008, the Dana-Farber Cancer Institute in Boston reported a two-year overall survival of about 53% and event-free survival of 70% (Chi et al., 2009). In 2013, the medical university in Vienna reported a 5-year overall survival of 100% and event-free survival of about 89% (Slavc et al., 2014). In Korea, the effectiveness of high dose chemotherapy combined with autologous stem cell transplantation technique was evaluated in children with AT/RT with a 3-year overall survival rate of about 53% ± 17%, which increased to about 80% after initiation of radiation treatment (Sung et al.,

2007). Hence, survival rates can be significantly improved with the correct genetic diagnosis followed by specific multimodal treatment.

AT/RT and rhabdoid tumors share the term "rhabdoid" because when checked under the microscope, both tumors resemble rhabdomyosarcoma, another malignant tumor that develops in the skeletal muscles and has failed to differentiate fully Morgenstern, Gibson, Brown, Sebire, and Anderson (2010). The tissue of this tumor contains different types of cell, including the rhabdoid cells, epithelial and mesenchymal cells, and large spindle-shaped cells. Most AT/RT's can be caused by changes in a gene known as SMARCB1 (Han et al., 2016; Pawel, 2018; Zimmermann & Zimmermann, 2016). This gene functions by providing instructions for making a protein that forms a subunit for a protein group called SWI/SNF complex. This complex regulates gene expression by a process called chromatin remodeling (L. Ho & Crabtree, 2010; Tang, Nogales, & Ciferri, 2010). It is how gene expression is regulated during development. However, in the case of AT/RT, SMARCB1 does not function properly and leads to uncontrolled tumor growth. This tumor is the first brain tumor in which a candidate tumor suppressor gene has been identified (Richardson, Ho, & Huang, 2018).

Various types of prognosis techniques are available, including tumor recognition, molecular classification, surgery, chemotherapy, and radiotherapy (Arruebo et al., 2011; Sawyers, 2004). However, each has its shortcomings, which highlights the importance of multimodality management in patients with AT/RT. A critical step in treatment planning is to determine the histology of the tumor. Misidentification of the tumor histology can lead to errors in prognosis and future treatments (Lee et al., 2017).

Cytogenetic studies can further assist in differentiation between medulloblastoma's and primitive neuroectodermal tumor (PNET), from AT/RT. Surgery plays a crucial role in obtaining tissues and makes an accurate diagnosis. However, surgery alone is not curative. More than 50% of the AT/RT tumors would respond to chemotherapy, and while there are no standard treatments known for AT/RT, specific agents that are used against CNS tumors include cisplatinum, carboplatinum, cyclophosphamide, vincristine, and etoposide (Biswas, Kashyap, Kakkar, Sarkar, & Julka, 2016). Hence, chemotherapy is an essential attribute in treating AT/RTs in young patients.

Intratumoral genetic heterogeneity is a widely accepted characteristic of human cancer, including various malignant brain tumors such as glioblastoma (Parker et al., 2018) and AT/RT (Johann et al., 2016). Brain tumors are the leading cause of mortality, and they remain difficult to cure despite advances in surgery and chemotherapy, because of their unclear cellular origin (Dirks, 2010). One of the current concepts in neuro-oncology is that brain tumors arise from a rare population of undifferentiated cells that may be similar to normal neural stem cells (NSCs). These cells have been termed as brain tumor stem cells (BTSCs) or brain tumor-initiating cells (BTICs) (S. A. Choi, Lee, et al., 2014; Germano, Swiss, & Casaccia, 2010; Swartling, Čančer, Frantz, Weishaupt, & Persson, 2015). These small population of cells has shown to express aldehyde dehydrogenase (ALDH), which is a polymorphic enzyme responsible for the oxidation of aldehydes to carboxylic acids (Koppaka et al., 2012; Marcato et al., 2011). They also play a role in the oxidation of retinol to retinoic acid in the early stem cells differentiation (Yoshida, Hsu, & Davé, 1992). ALDH activity, which can be easily

measured using an Aldefluor assay, is now used as one of the Cancer Stem cell (CSC) markers for many cancers. We previously reported that primary brain tumors contain distinct subpopulations of cells that have high expression levels of ALDH and BTIC characteristics (S. A. Choi, Lee, et al., 2014; Ginestier et al., 2007). In that study, the ALDH+ fraction tended to be higher in aggressive tumors, such as AT/RT. Furthermore, we found that the targeted knockdown of ALDH1 by short hairpin RNA in BTICs potently disrupted their self-renewing ability (S. A. Choi, Lee, et al., 2014).

Disulfiram (Antabuse) was the first drug approved by the U.S. Food and Drug Administration to treat chronic alcohol dependence (Mutschler, Grosshans, Soyka, & Rösner, 2016). The drug has a strong affinity for protein-bound and unbound thiols and forms a covalent linkage with an active-site cysteine of the aldehyde dehydrogenase (ALDH) to inactivate the enzyme and build up the acetaldehyde concentrations to cause aversion to alcohol. Recently, it has gained prominence as a potent anticancer drug, owing to its pharmacological actions on multiple targets in tumor cells such as breast cancer (Chen, Cui, Yang, & Dou, 2006), head and neck cells (Y. M. Park et al., 2018), lung cancer cells (Nechushtan et al., 2015). It has been shown to trigger oxidative stress by generating reactive oxygen species (ROS) (Zha et al., 2014) and activate the mitogen-activated protein kinase (MAPK) pathway and affect the NF κB pathway (Yip et al., 2011). It has also shown to inhibit proteasomes (Cvek, 2011) and DNA topoisomerase (Yakisich, Sidén, Eneroth, & Cruz, 2001). Disulfiram can reverse the resistance to chemotherapy drugs by inhibiting the P-glycoprotein (Pgp) multidrug efflux pump (Cvek, 2011). It has also been reported to target ALDH positive cells in

brain tumor-initiating cells within AT/RT both *in vitro* and *in vivo* (S. A. Choi, Choi, et al., 2014; Hanumantha Rao Madala, Ali-Osman, Zhang, & Srivenugopal, 2018). Interestingly, it also potentiates cyclophosphamide, cisplatin, and radiation *in vitro* and protects the normal cells in kidneys and bone marrow while increasing the therapeutic index of cytotoxic drugs (Bodenner, Dedon, Keng, Katz, & Borch, 1986; Hacker, Ershler, Newman, & Gamelli, 1982). This study worked at confirming the tumor-suppressive effects of disulfiram targeting ALDH expression, which is abundant in AT/RTs (S. A. Choi, Choi, et al., 2014).

The past century has demonstrated that cancer can be effectively treated with surgery, chemotherapy, and radiotherapy. These treatment strategies, either alone or in combination, can significantly impact tumor growth or possibly even produce cures. For solid tumors, improved methods for early diagnosis have an important impact on survival. However, once the tumor has metastasized, treatment becomes more complicated (Shewach & Kuchta, 2009). Various chemotherapeutic agents have already been used against CNS tumors, including cisplatin, carboplatin, cyclophosphamide, vincristine, and etoposide.

Platinum-based chemotherapy regimens continue to be a part of mainstream treatment techniques for multiple solid tumors, including AT/RT (Galanski, 2006; Hill & Speer, 1982; Lafay-Cousin et al., 2012). Since its introductions into clinical trials in 1971 and subsequent FDA approval in 1978,cis-diammine-dichloro-platinum II (cisplatin) represents a major landmark in the history of successful anti-cancer therapeutics (Kelland, 2007). It functions by DNA crosslinking that leads to impaired

transcription and replication and ultimately cell cycle arrest and apoptosis (Neuwelt et al., 2014). Cisplatin covalently binds DNA to form bulky adducts that block replication and transcription, which leads to G2 phase cell cycle arrest. Cisplatin has pleiotropic effects on the cell and investigating cellular pathways of cisplatin cytotoxicity may lead to the development of novel targeted therapies. For example, the mitogen-activated protein kinase (MAPK) cascade is an extracellular stress response pathway that includes three kinase members: extracellular signal-regulated kinase (ERK), c-Jun *N*-terminal protein kinase (JNK), and p38, all of which are activated by cisplatin (Siddik, 2003). This pathway is important for the cytotoxic action of cisplatin since inhibition of any member can attenuate cisplatin-induced apoptosis (Brozovic & Osmak, 2007; Yeh et al., 2002).

But while these platinum-based drugs are effective, its use is limited by severe dose-limiting side effects which include nephrotoxicity for cisplatin and myelosuppression for carboplatin, etc. (Oun, Moussa, & Wheate, 2018). Also, the development of cisplatin resistance has become a major challenge in the treatment and management of brain tumor patients. Alternative strategies to overcome cisplatin resistance are of critical importance in order to enhance the current therapeutic efficacy of this chemotherapeutic drug. Furthermore, patients require extensive monitoring for their biochemistries and kidney and liver function. Therefore, patients are commonly co-prescribed additional chemotherapeutic drugs that can reduce the cytotoxicity of such drugs.

The idea of combination therapy arrived in the 1960s and resulted in tremendous improvements in patient outcome. Researchers believe that one possible way to overcome or delay the development of resistance is to treat patients with a combination of different drugs. One of the treatments includes the co-administration of different drugs affecting different molecular mechanisms, thereby increasing the tumor cell death and reduce any chances of drug resistance and overlapping toxicity (Al-Lazikani, Banerji, & Workman, 2012). Currently, nearly all chemotherapeutic regimens involve a cocktail of drugs. The combination of cisplatin and disulfiram has been used in various other solid tumors such as breast cancer, prostate cancer and ovarian cancer (O'Brien, Barber, Reid, Niknejad, & Dimitroulakos, 2012; Papaioannou, Mylonas, Kast, & Brüning, 2014). In attempts to find a standard chemotherapeutic strategy for AT/RT tumor, we used disulfiram and combined it with an existing AT/RT drug, cisplatin. This approach targeted not only the ALDH positive population within AT/RT cells but also the other heterogeneous bulk cell population (Schatton, Frank, & Frank, 2009).

Presently, our target was to understand the shortcomings associated with conventional chemotherapeutic drugs (cisplatin, etoposide, and cyclophosphamide (4-HC)) and how disulfiram can work to enhance tumor cell apoptosis when given in combination with these drugs. Amongst the existing drugs, we chose cisplatin as our drug of interest and confirmed its effects both singularly and in combination with disulfiram. While understanding the potential mechanism associated with this drug combination, we also noticed the importance of the DNA damage proteins and ATF3 that was affected by our drug combination and how it synergistically activated apoptosis via

cleaved PARP. This study demonstrates not only the enhanced effects of conventional drugs when combined with ALDH inhibiting drug, but also highlights a potential pathway that leads to cell apoptosis in tumor cells.

Materials and Methods

1.1. Cell cultures

AT/RT surgical samples were derived from patients undergoing treatment in Seoul National University Children's Hospital upon receiving appropriate written consent by the institutional review board (IRB #1801-117-917). The cells were cultured from the surgical samples (Table 1) and the established AT/RT cell lines, BT12, and BT16 were received from Nationwide Children's Hospital. All AT/RT cells were cultured in Dulbecco's modified Eagle's medium (DMEM) containing 10% fetal bovine serum and 1x antibiotic-antimycotic. Cells were incubated at 37° C temperature and 5% CO_2 in an incubator (S. A. Choi et al., 2012). AT/RT primary cultured cells (SNUH.AT/RT05, SNUH.AT/RT08, SNUH.AT/RT09, and SNUH.AT/RT11) under the passage number 7 were used in all experiments in this study.

Table 1. Patient information

Sample	Gender	Age	Subtype	Surgery Type
SNUH.AT/RT05	M	20m	TYR/MYC	MLSOC and NTR
SNUH.AT/RT08	M	11m	TYR/MYC	craniotomy and GTR
SNUH.AT/RT09	F	2m	TYR/MYC	MLSOC and STR
SNUH.AT/RT11	M	9m	SHH	OTT and GTR

1.2. Cell viability analysis

Disulfiram and cisplatin were purchased (Selleckchem, Texas, USA) and stock solutions were prepared (100 μM) in DMSO for disulfiram and DMEM for cisplatin, respectively. We assessed the cell viability by EZ−Cytox, (DAEIL Lab, Seoul, Korea) 4 x 10^3 cells were seeded into a 96−well plate with 100 μl of DMEM media per well and incubated for 24 hours. For single drug treatment, the cells were exposed to increasing concentrations of drug doses from 0 to 100 μM final concentration for 48 hours, 72 hours, and 96 hours, respectively. The inhibitory concentration of 50% (IC_{50}) of disulfiram and cisplatin was determined using Prism software. After IC_{50} calculation, the effectiveness of the drug doses was also confirmed *in vitro* by treating cells after 4 hours of each other and concomitantly and an isobologram calculated via CompuSyn software. The viable cells were measured at 450 nm using a spectrophotometer. The results are shown as a percentage of cell viability in treated cells compared with untreated control.

1.3. Fluorescence-activate cell sorting (FACS)

The amount of ALDH positive cells ($ALDH^+$) within AT/RT, were analyzed using ALDEFLOUR assay kit (Aldagen, Inc. Durham, USA) (S. A. Choi, Lee, et al., 2014). Briefly, cells were suspended in Aldefluor assay buffer containing ALDH substrate, BAAA (1 μmol/L) for 40 min per 1 x 10^6 cells. For each experiment, the samples were stained under identical conditions with 50 mmol/L of specific ALDH inhibitor diethyaminobenzaldehyde (DEAB) as a negative control. Flow cytometric sorting was conducted using a FACS Aria. (Becton Dickinson Immunocytometry System, Mountain

View, CA) Aldefluor fluorescence was calculated at 488 nm, and fluorescence emission detected using a standard fluorescein isothiocyanate (FITC) 530/30−nm band pass filter by a FACS caliber machine (BD Biosciences, San Jose, CA) High side scatter ALDH1+ and low ALDH1− were selected.

1.4. Enzyme-linked immunosorbent assay (ELISA)

Proteins were extracted using radioimmunoprecipitation assay (RIPA) buffer used to measure the ALDH activity assay, performed according to the manufacturer's protocol (Abcam − 155893). The NAD−dependent Aldehyde Dehydrogenase (ALDH) plays an essential role in cellular detoxification. It can oxidize various aldehydes and generate the corresponding carboxylic acid. Cell lines and primary cultured cells (2×10^6) were tested for NADH generated by acetaldehyde after it has been oxidized by ALDH present in the cells. The ALDH activity was measured at two−time points of 1 hr, and 2 hrs post−treatment and data calculated according to protocol. End products were tested at 450nm absorbance, respectively. The ALDH activity was expressed in nmol/min/ml.

1.5. Western blot

Cells (1×10^6) containing proteins were lysed using RIPA buffer, and 30μg of proteins were used for western blot analysis. Cells were treated for 24 h, and the analysis performed. Primary antibodies were used against ATF3 (1:100, Cell Signaling), P38 and Phospho P38 (1:1000, Abcam), C−Jun and Phospho C−Jun (1:1000, Abcam), p53 (1;500, Abcam), Cleaved PARP (1:1000,Abcam), Survivin (1:5000,Abcam), γ−H2AX (1:2000,Abcam), DNA−PKcs (1:1000,Abcam) and β−actin (1:5000,Sigma−Aldrich).

Band density was analyzed via Image J software. Data were normalized according to their corresponding β-actin levels (S. Choi et al., 2015).

1.6. Orthotopic AT/RT xenograft mouse model

All the animals in the experiments were approved by the Institutional Animal Care and Use Committee (IACUC number 18-0020-C1A0 at the Seoul National University. Seven-week-old female BALB/c-nude mice were anesthetized by intraperitoneal (i.p.) injection of 30mg/kg Zoletil and 10mg/kg Xylazine. BT16 expressing luciferase (BT16-effluc) were used for bioluminescence imaging, as described previously (Lee et al., 2017). BT16-effluc cells (1.2×10^5 in 3 μl of PBS) were injected via a stereotaxic device into the brains, using a Hamilton syringe at the injection rate of 1μl/min. Stereotaxic coordinates were chosen to be 1mm anterior and 2mm lateral to the bregma and at 3mm depth from the dura. For long term survival model, N = 10 mice were used for each group and short term and immunofluorescence analysis model, N = 4 mice per group were used with a total of 4 experimental groups; saline (control group), disulfiram treated group, cisplatin-treated group, and a combination of disulfiram and cisplatin-treated group.

1.7. Drug treatment *in vivo*

Seven days post-injection of BT16-effLuc cells, the mice were randomly sorted into groups. The mice were injected i.p. with saline for the control group, 25mg/kg disulfiram for 5 consecutive days and 5mg/kg of cisplatin twice, for a period of two weeks as indicated in the treatment scheme (Figure 10) The disulfiram dose was determined as a quarter of the effective dose (100mg/kg) (S. A. Choi, Choi, et al., 2014; Lee et al.,

2017). On first-day, post disulfiram treatment in the left flank, cisplatin treatment was given in the right flank and injections of both drugs given to the disulfiram+cisplatin group mice, one after the other, in succession.

1.8. *In vivo* live imaging and survival analysis

Brain tumor growth was monitored via bioluminescence imaging using IVIS-100 (Xenogen) systems followed by imaging every seven days until day 63 post-injection. The mice received an i.p administration of 150mg/kg D-Luciferin (Caliper Life sciences) and then were anesthetized with 2% isoflurane (Piramal Healthcare) in 100% O_2. Images were acquired by recording the bioluminescent signal for 1-3mins and were analyzed via Living Image Software (Xenogen). The signal was quantified by calculating the luminous intensity in the region of interest. All the animals were imaged until euthanasia or the survival endpoint of 120 days.

1.9. Histological analysis

The mice were sacrificed for histological analysis 54 days after tumor cell injection. Cardiac perfusion was performed, and frozen blocks were prepared for sectioning. The entire brain was placed in 4% paraformaldehyde for 24 hours and serially dehydrated in 10%, 20% and 30% sucrose for cryosectioning. The tissues obtained were embedded in Tissue-Tek Optimal Cutting temperature compound (OCT) and frozen at -70° C. The tissues were sectioned in the axial plane at 10μm using a cryotome and stained with hematoxylin and eosin (H&E) for histopathologic examination. Post-treatment the sections were washed with PBS and counter-stained with aqueous eosin for 30 seconds.

Finally, the sections were dehydrated in ascending series of ethanol (70%, 95%, and 100%) and passed through xylene and then mounted.

1.10. Immunofluorescence staining

Sectioned tissues were treated in permeabilization buffer for 15 mins and blocking buffer for 20 mins. The sections were incubated with primary antibodies ALDH1a1 (1:100, Abcam, Cambridge, USA), pDNA-PKcs (1:1000, Abcam, Cambridge, USA), γ H2Ax (1:100, Abcam, Cambridge, USA), ATF3 (1:50, Santa Cruz Biotechnology, TX, USA) and Cleaved PARP (1:400, Abcam, Cambridge, USA) for 18 hours at 4° C and rinsed using PBS the secondary antibody used was Alexa Fluor 594 or 488- conjugated with anti-rabbit IgG (1:500; Invitrogen) or 594-conjugated anti-goat IgG (1;500, Invitrogen) was used and the sections were mounted with antifading solution containing DAPI. Fluorescent images were obtained using confocal microscopy. Quantification of positively stained slides was performed from a minimum of three randomly stained slides.

Results

2.1. Synergistic effect of disulfiram and cisplatin in combination treatment

We confirmed the IC_{50} of disulfiram with different conventional chemotherapeutic drugs such as cisplatin, etoposide, and 4HC (4-hydroperoxycyclophosphamide). To compare the anticancer effect of disulfiram combinations with these drugs, we first treated primary cultured cells (SNUH.AT/RT 05, SNUH.AT/RT08, SNUH.AT/RT09 and SNUH.AT/RT11) established cell lines (BT12 and BT16) and HB1.F3 which are human neural stem cells, with a dose range of 0 to 100 μM drug respectively. The IC_{50} values of these drugs were obtained via a dose-response curve. (Figure 1 and Table 2)

Disulfiram was seen to be affecting cells at low doses for almost all cells except SNUH.AT/RT11. While cisplatin and etoposide had an IC_{50} range from 5 to 45 μM, 4HC had a high drug concentration range of 7 to 74 μM. HB1.F3 or normal neural stem cells had an IC_{50} concentration of 34 μM, 60 μM, 80 μM and 37 μM for disulfiram, cisplatin, etoposide and 4HC respectively, which is higher than cell lines and primary cultured cells for disulfiram, cisplatin and etoposide but lower than some cases of primary cultured cells for 4HC drug (Table 2). Further analysis showed that cisplatin when combined in serial drug doses with disulfiram, lead to synergistic effects with an IC_{50} effect or lower at 20μM each for SNUH.AT/RT09 and SNUH.AT/RT11 while for cell lines at 5μM of drug combination (Figure 2 and Table 3). While etoposide did not show synergism at serial dilution doses for SNUH.AT/RT08 and had a high synergistic effect of 20 μM each for BT12. (Figure 3 and Table 4). To confirm the synergistic effect of cisplatin with disulfiram an isobologram was constructed (Figure 5). It was also

observed that drug combinations when given after 4 hours of each other were still more effective than control and single treatment, but the effectiveness increased when both drugs were given concomitantly to the cells. ($p<0.001$) (Figure 4).

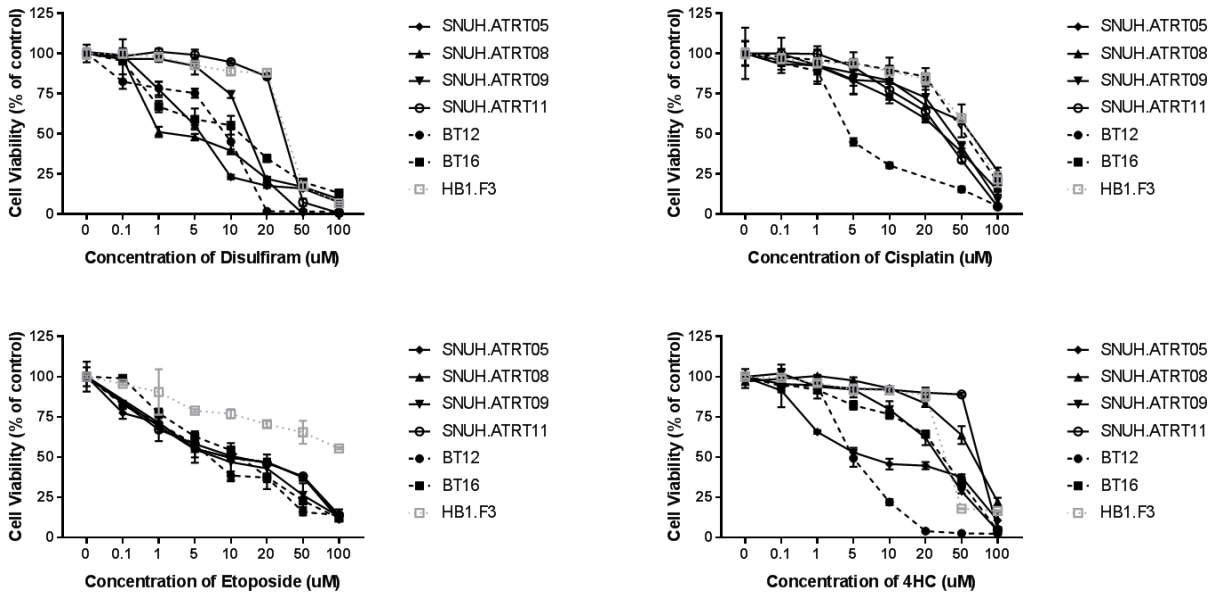

Figure 1. Cell viability of disulfiram with conventional drugs.

Cells were treated with increasing concentrations of disulfiram, cisplatin, etoposide, and 4HC. Cell viability was decreased, disulfiram was more effective than the other drugs in different ATRT positive cells and cell lines (IC_{50}– 5 ± 0.8 in SNUH.AT/RT05, 4 ± 2 in SNUH.AT/RT08 and 12.8 ± 4 in SNUH.AT/RT09 and for established cell lines 12 ± 1.05 in BT12 and 5 ± 0.1 in BT16 respectively)

Table 2. Half-Maximal Inhibitory Concentration (IC_{50}), μM

Cell lines	Disulfiram	Cisplatin	Etoposide	4-HC
SNUH.AT/RT05	5.0	30.0	12.0	10.0
SNUH.AT/RT08	4.0	45.0	16.0	26.0
SNUH.AT/RT09	12.0	34.0	18.0	55.0
SNUH.AT/RT11	30.0	40.0	16.0	74.0
BT12	12.0	5.0	20.0	7.0
BT16	5.0	40.0	15.0	19.0
HB1.F3	34.0	60.0	80.0	37.0

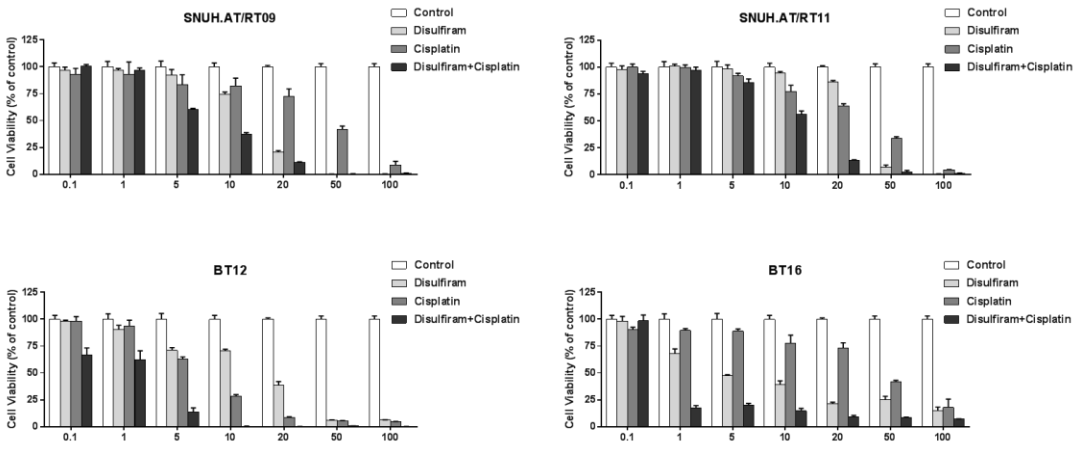

Figure 2. Cell viability of disulfiram with cisplatin confirming the IC_{50}

Primary cultured and established cell lines were given fixed drug doses of disulfiram and cisplatin ranging from 0.1 to 100μM, respectively. The synergistic effects of the drugs in combination were computed via CompuSyn software. Drug dose with the most synergistic effect and overall disulfiram+cisplatin combination less than IC_{50} were chosen for further experiments. (20μM for SNUH.AT/RT09 and SNUH.AT/RT11 and 5μM for BT12 and BT16 respectively)

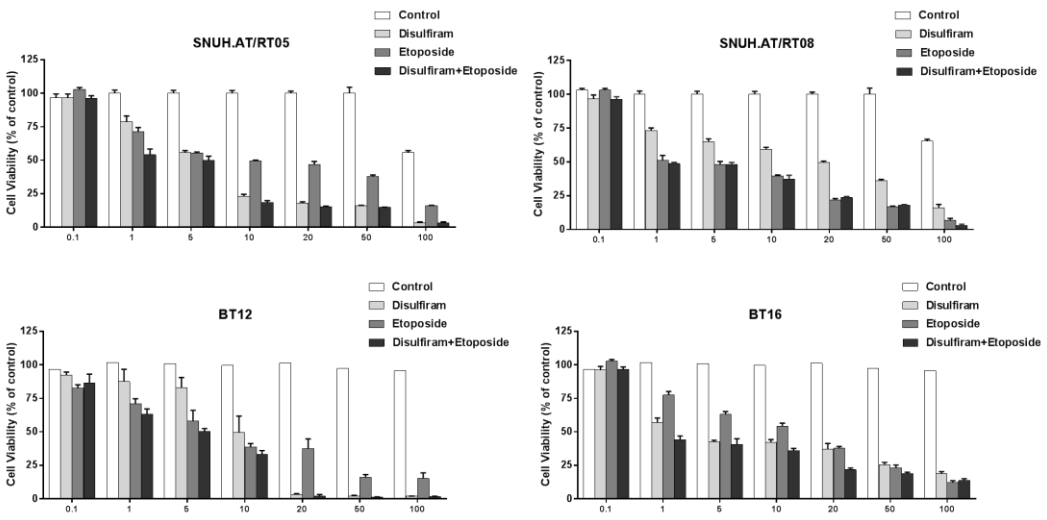

Figure 3. Cell viability of disulfiram with etoposide confirming the IC_{50}

Primary cultured and established cell lines were given fixed drug doses of disulfiram and etoposide ranging from 0.1 to 100μM, respectively. The synergistic effects of the drugs in combination were computed via CompuSyn software. While no synergism was found in SNUH.AT/RT08, 10μM was found for SNUH.AT/RT05 and 20μM and 5μM were found for BT12 and BT16 respectively)

Table 3. CI value calculation for cisplatin in combination with disulfiram, (μM)

Cells	Disulfiram	Cisplatin	Total Dose	CI value	Interpretation
SNUH.AT/RT09	0.1	0.1	0.2	0.36047	Synergistic
	1.0	1.0	2.0	2.03542	Antagonistic
	5.0	5.0	10.0	1.53124	Antagonistic
	10.0	10.0	20.0	1.58065	Antagonistic
	20.0	20.0	40.0	1.07209	Additive
SNUH.AT/RT11	0.1	0.1	0.2	0.09834	Synergistic
	1.0	1.0	2.0	0.62006	Synergistic
	5.0	5.0	10.0	1.61431	Antagonistic
	10.0	10.0	20.0	1.15784	Antagonistic
	20.0	20.0	40.0	0.57472	Synergistic
BT12	0.1	0.1	0.2	0.08257	Synergistic
	1.0	1.0	2.0	0.67906	Synergistic
	5.0	5.0	10.0	0.4546	Synergistic
	10.0	10.0	20.0	0.29029	Synergistic
	20.0	20.0	40.0	0.57993	Synergistic
BT16	0.1	0.1	0.2	1.17665	Antagonistic
	1.0	1.0	2.0	0.07475	Synergistic
	5.0	5.0	10.0	0.19844	Synergistic
	10.0	10.0	20.0	0.31965	Synergistic
	20.0	20.0	40.0	0.32895	Synergistic

Table 4. CI value calculation for etoposide in combination with disulfiram, (μM)

Cells	Disulfiram	Etoposide	Total Dose	CI value	Interpretation
SNUH.AT/RT05	0.1	0.1	0.2	2.67152	Antagonistic
	1.0	1.0	2.0	0.49974	Synergistic
	5.0	5.0	10.0	1.57004	Antagonistic
	10.0	10.0	20.0	0.38700	Synergistic
	20.0	20.0	40.0	0.60286	Synergistic
SNUH.AT/RT08	0.1	0.1	0.2	2.51453	Antagonistic
	1.0	1.0	2.0	0.49514	Synergistic
	5.0	5.0	10.0	2.29471	Antagonistic
	10.0	10.0	20.0	1.76025	Antagonistic
	20.0	20.0	40.0	1.2051	Antagonistic
BT12	0.1	0.1	0.2	1.11263	Antagonistic
	1.0	1.0	2.0	1.22503	Antagonistic
	5.0	5.0	10.0	2.8165	Antagonistic
	10.0	10.0	20.0	2.24597	Antagonistic
	20.0	20.0	40.0	0.19004	Synergistic
BT16	0.1	0.1	0.2	3.76709	Antagonistic
	1.0	1.0	2.0	0.16533	Synergistic
	5.0	5.0	10.0	0.69576	Synergistic
	10.0	10.0	20.0	1.10682	Antagonistic
	20.0	20.0	40.0	1.07777	Additive

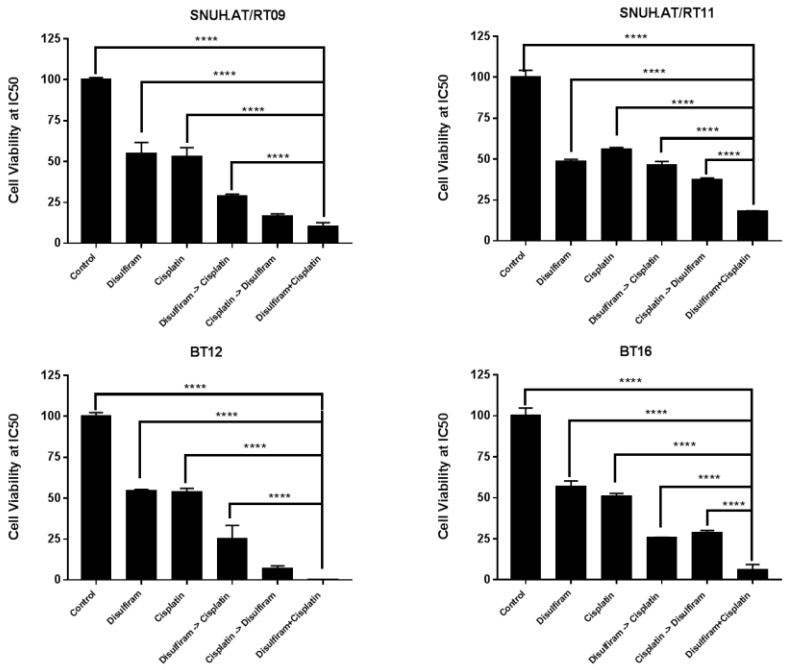

Figure 4: Drug treatment at different time intervals.

Disulfiram and cisplatin were treated as a single treatment, after 4 hours of each other and concurrently to determine drug effectiveness. It was observed that drug combinations of disulfiram and cisplatin when given 4 hours from each other were still more effective than control and single treatment, but drug affectivity increased when both drugs were given simultaneously to the cells *in vitro*. (**** $p<0.001$).

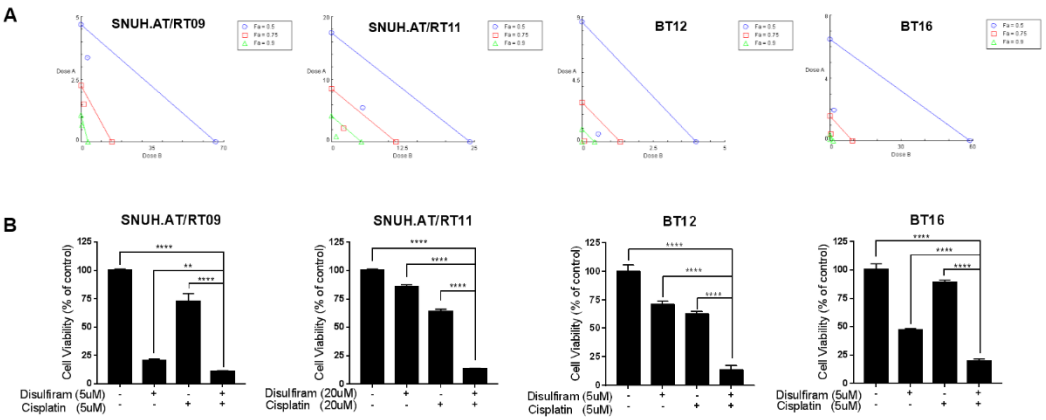

Figure 5: Synergistic effect of disulfiram and cisplatin on primary cultured cells and established cell lines

The synergistic effects of disulfiram and cisplatin were calculated via (A) Isobologram analysis as well as via (B) cell viability test. Both cells showed a decrease in cell viability when comparing control v/s combination in primary cultured cells. (****p<0.001 in both SNUH.AT/RT09 and SNUH.AT/RT11 cells. While BT16 cell line showed resistance to cisplatin, single treatment. Both cell lines also showed an overall decrease in cell viability. (****p<0.001 in both BT12 and BT16 cells)

2.2. Decreased ALDH enzyme activity by combination treatment

We have previously isolated spheroid cells from two different AT/RT tissues. We identified the distribution of ALDH+ cells within both primary cultured cells and established cell lines by FACS analysis. Primary cultured cells contained 3.05% ALDH positive cells in SNUH.AT/RT09 and 5.57% in SNUH.ATR/T11 cell, respectively. We also tested for ALDH positive cells in established cell lines, which amounted to 2.21% in BT12 and 2.95% in BT16 cells (Figure 6). We targeted these small cell populations within the tumor by an ALDH inhibitor, disulfiram, and also tested its effects when in combination with cisplatin. The primary cultured cells and cell lines were incubated at 20μM and 5μM drug combinations respectively. ALDH enzyme activity was confirmed for the control group, single treatment groups, and combination treatment group. Primary cultured cells, SNUH.AT/RT09 and SNUH.AT/RT11 showed an expression level of 0.06 ± 0.05 and 0.06 ± 0.04 nmol/min/ml respectively for combination treatment group while BT12 and BT16 had an expression level of 0.07 ± 0.02 and 0.24 ± 0.05 nmol/min/ml respectively for combination treatment as compared to a range of control values at 1.05 ± 0.5 to 1.33 ± 0.6 nmol/min/ml, detected at 450nm and calculated according to the formulas provided in the protocol (Figure 7).

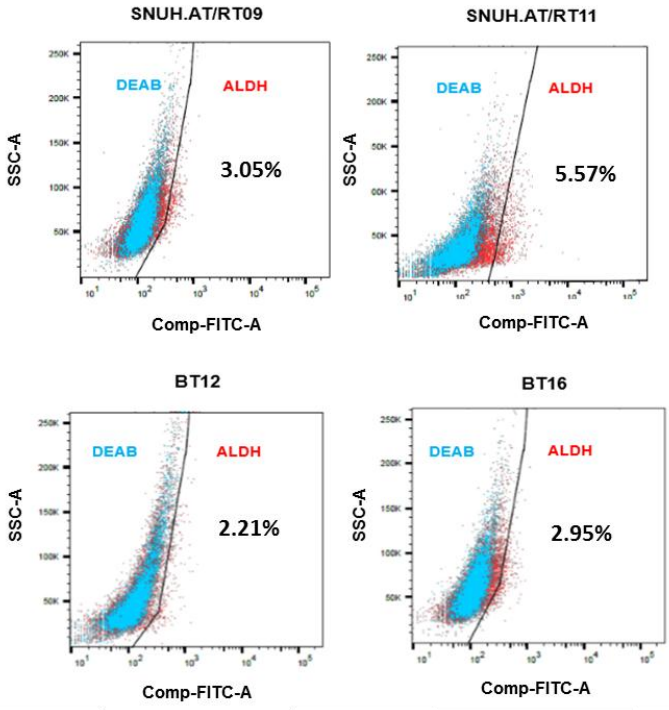

Figure 6: ALDH positive cell population in primary cultured cells and established cell lines

Cells were incubated with Aldefluor substrate (BAAA). The brightly fluorescent ALDH1− expressing cells were detected in the FITC channel. Diethylaminobenzaldehyde (DEAB) was used as an ALDH blocking reagent. Primary cultured cells expressed ALDH1 ranged from 3.05% to 5.57% while for cell lines it ranged from 2.21% to 2.95%)

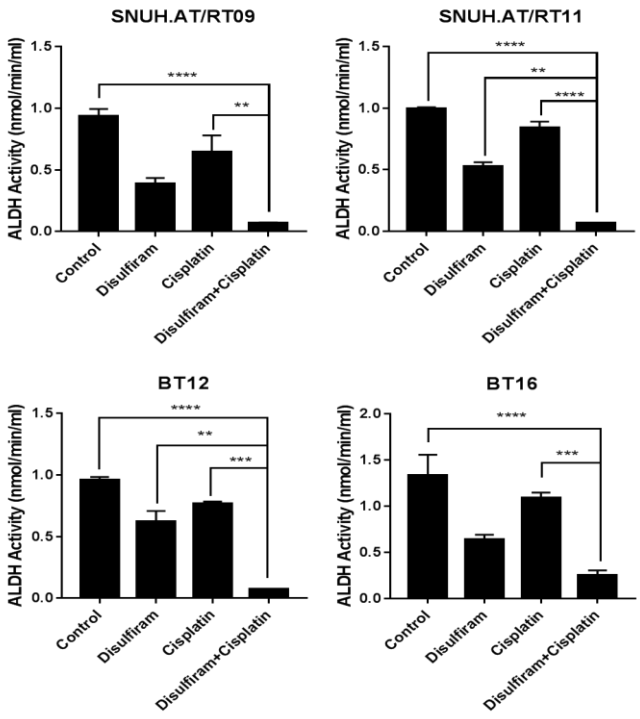

Figure 7: ALDH enzyme activity in primary cultured cells and established cell lines

ALDH enzyme activity within each cell was calculated by adding acetaldehyde and checking the NADH conversation rate after a time point of 1 hour and 2 hours, respectively. The absorbance was calculated at 450nm. BT12 and BT16 had an ALDH expression level of 0.07 ± 0.02 and 0.24 ± 0.05 nmol/min/ml respectively. While primary cultured cells showed an expression level of 0.07 ± 0.05 and 0.064 ± 0.04 nmol/min/ml respectively compared to control values of 1.61 ± 0.6 nmol/min/ml. (**p−0.0373,***p−0.0007,****p<0.0001)

2.3. Regulation of ATF3 leading to apoptosis in AT/RT cells

Based on the predicted mechanisms that work to accentuate the synergism between disulfiram and cisplatin (Figure 8), we examined the protein expressions related to ATF3 regulation, p53 activation, c-Jun pathway, and DNA damage proteins associated with cellular apoptosis in primary cultured cells and established cell lines. In the case of ATF3 protein, it was significantly upregulated when comparing control and single treatment groups with that of combination. For the phosphorylated form of cJun protein for SNUH.AT/RT09, SNUH.AT/RT11 and BT12 had some significant effect *in vitro* (Figure 9 and Figure 10). While in the case of p38 protein no significance was observed for both p38 antibody and its phosphorylated form. p53 is a tumor protein was expressed significantly in SNUH.AT/RT09 and BT16 with at least an additive effect in SNUH.AT/RT11 and BT12 respectively. Cleaved PARP that leads to apoptosis *in vitro* was seen to be highly expressed in the combination group and was significantly upregulated (Figure 10). Survivin that is p53 independent and works downstream of it were seen to have a decreased expression. pDNA-PKcs which is a DNA damage marker and γ-H2AX, a DNA double-strand break marker were both observed to have an increased expression for combination drug doses in all cell lines further confirming effective apoptosis *in vitro*.

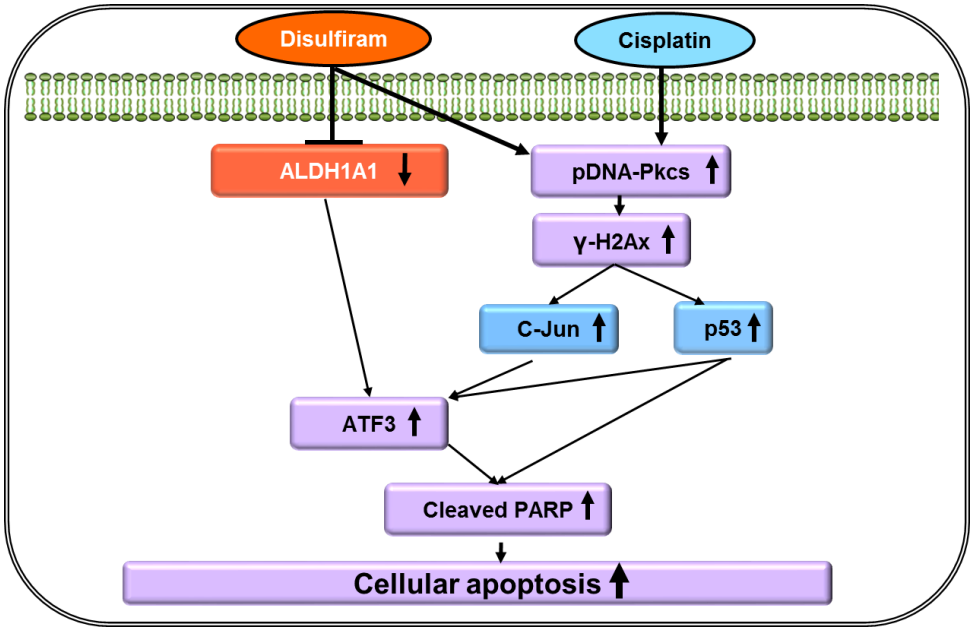

Figure 8: Predicted mechanism of ATF3, c−Jun, p53 and ALDH1A1 pathway affected by disulfiram and cisplatin working in synergism

ALDH1A1 is connected by ATF3 and pDNA−PKcs, which further affects γ H2Ax, while cisplatin also affects these DNA damage proteins and significantly affects both ATF3 and cleaved PARP downstream leading to cellular apoptosis.

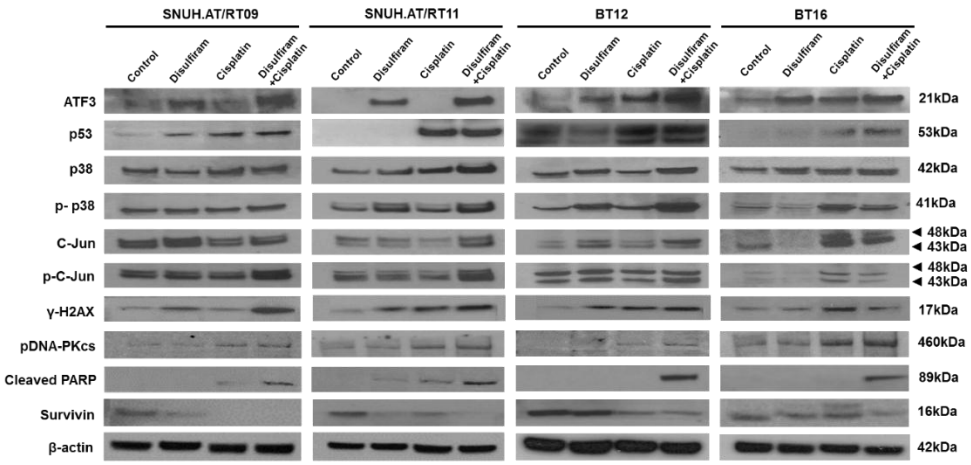

Figure 9: Western blot analysis in AT/RT cells

Both disulfiram and cisplatin were seen to affect ALDH1 pathway as well as p-cJUN and p53 which significantly affect AT/RT cells, which further leads to activation of ATF3 downstream. This further activated cleaved PARP and lead to apoptosis within the cells. Other DNA damage proteins and apoptosis proteins like pDNA-PKcs, γH2Ax and survivin were also seen to be upregulated in the combination group.

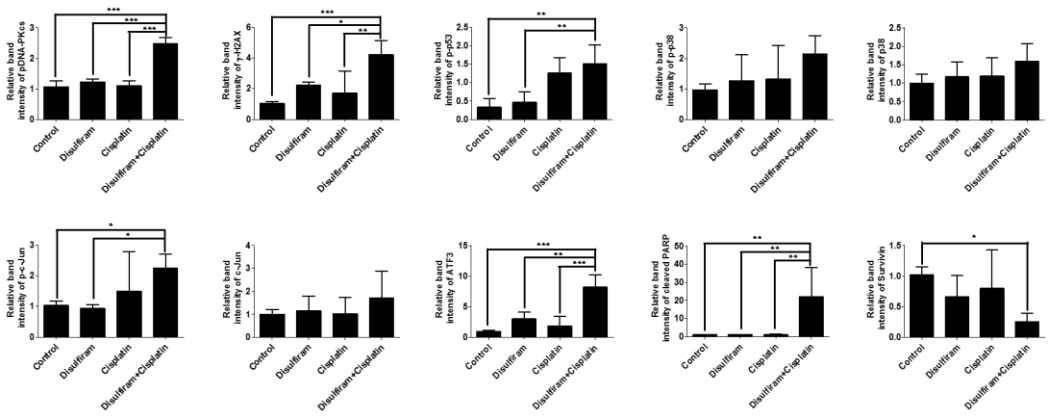

Figure 10: Quantification of western blot proteins

ALDH expression was downregulated while the other proteins were upregulated *in vitro*. There was a significant effect seen for pDNA−PKcs, γH2Ax, ATF3, and cleaved PARP. In the case of survivin, the cells that survived least as compared to control and single treatment were from the disulfiram+cisplatin group.

2.4. Increased survival in long term *in vivo.*

The AT/RT animal models and treatment schemes are shown in Figure 11. The results show that the mice were more sensitive to cisplatin single treatment with overall survival of 37 days and a drastic drop in body weight, which is even lower than control mice, which had a median survival of 60 days. Disulfiram single treatment drug was well tolerated in mice and had a median survival of 69 days and maintained their bodyweight post−treatment (Figure 12 and Figure 13), but was not very effective in reducing bioluminescence signal in comparison to cisplatin single treatment. Disulfiram and cisplatin bioluminescence imaging quantification at day 49 post−treatment versus combination were at 1.E+07 ± 3.E+06 and 2.E+07 ± 1.E+06 v/s 4.E+06 ± 1.E+06 respectively. While that of control versus combination was at 2.E+07 ± 2.E+06 v/s 4.E+06 ± 1.E+06 (Table 5). The long term medial survival results showed that disulfiram+cisplatin combination not only survived longer in comparison to single−drug treatment groups at a survival rate of 75 days but also had a reduced bioluminescence signal (Figure 12). The combination group mice also maintained body weights and lingered between cisplatin and disulfiram single treatment groups thereby affected by both drugs simultaneously (Figure 13). The overall survival significance is shown as follows, control with disulfiram+cisplatin: $p < 0.0001$; cisplatin with disulfiram+cisplatin: p−0.0002 and disulfiram with disulfiram+cisplatin: p−0.0273)

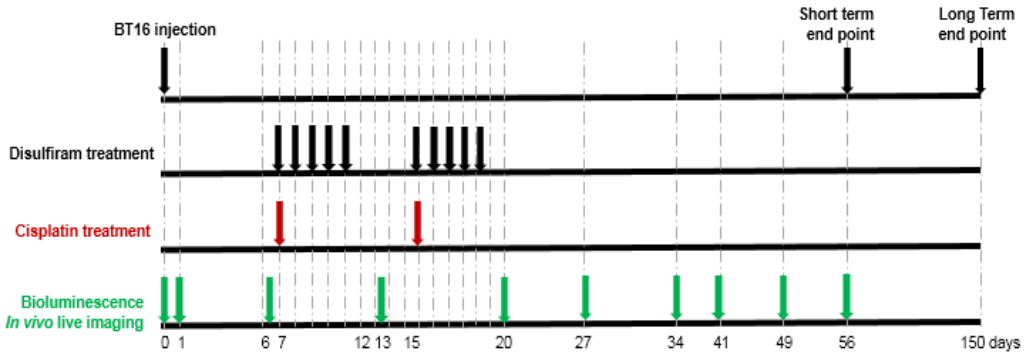

Figure 11: *In vivo* schematic diagram for drug treatment

An *in vivo* schematics of duration and time point for treatment and imaging for disulfiram and cisplatin are shown.

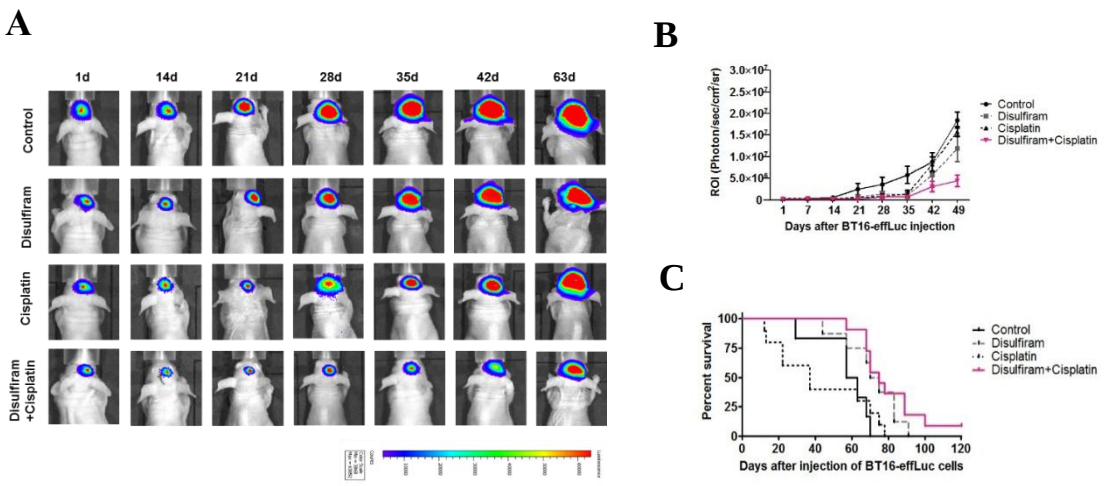

Figure 12: Long-term treatment effects of disulfiram and cisplatin combination therapy.

(A) Bioluminescence images (BLI) were obtained at various time points using an IVIS-100 imaging machine. (B) Tumor growth was quantified by BLI and compared for different drug doses and combination. (C) The median survival time of the groups (in days) was illustrated by Kaplan-Meier survival curves and compared using the log-rank test. Disulfiram+cisplatin combination group showed higher survival as compared to the control group at 75 days (p- <0.0001). While in case of single treatment, disulfiram treated mice survived for a total of 69 days (p- 0.0273) and cisplatin-treated mice showed drug sensitivity and had a shorter survival period of 37 days (p-0.0002)

Table 5. Quantification of tumor growth by bioluminescence image (BLI)

SEM	Control	Disulfiram	Cisplatin	Disulfiram+cisplatin
1	2.E+05 ± 3.E+04	3.E+05 ± 1.E+04	3.E+05 ± 5.E+04	3.E+05 ± 2.E+04
7	3.E+05 ± 3.E+04	3.E+05 ± 2.E+04	3.E+05 ± 3.E+04	3.E+05 ± 3.E+04
14	5.E+05 ± 9.E+04	2.E+05 ± 6.E+04	2.E+05 ± 2.E+05	2.E+05 ± 6.E+04
21	2.E+06 ± 1.E+06	6.E+05 ± 4.E+05	5.E+05 ± 3.E+05	2.E+05 ± 1.E+05
28	4.E+06 ± 2.E+06	1.E+06 ± 7.E+05	8.E+05 ± 6.E+05	6.E+05 ± 5.E+05
35	6.E+06 ± 2.E+06	1.E+06 ± 7.E+05	1.E+06 ± 8.E+05	7.E+05 ± 3.E+05
42	9.E±06 ± 2.E+06	6.E+06 ± 3.E+06	8.E+06 ± 2.E+06	3.E+06 ± 1.E+06
49	2.E+07 ± 2.E+06	1.E+07 ± 3.E+06	2.E+07 ± 1.E+06	4.E+06 ± 1.E+06

Table 6. p−value comparison analysis of region of interest (ROI) values

Days	Control vs Disulfiram+cisplatin	Disulfiram vs Disulfiram+cisplatin	Cisplatin vs Disulfiram+cisplatin
1	$p > 0.05$	$p > 0.05$	$p > 0.05$
7	$p > 0.05$	$p > 0.05$	$p > 0.05$
14	$p > 0.05$	$p > 0.05$	$p > 0.05$
21	$p > 0.05$	$p > 0.05$	$p > 0.05$
28	$p > 0.05$	$p > 0.05$	$p > 0.05$
35	$p < 0.05$	$p > 0.05$	$p > 0.05$
42	$p < 0.01$	$p > 0.05$	$p < 0.05$
49	$p < 0.001$	$p < 0.001$	$p < 0.001$

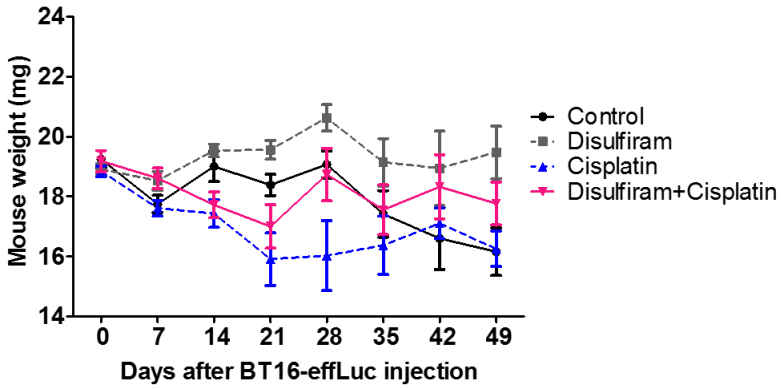

Figure 13: Comparison of body weight in BT16 effLuc mice model

Bodyweight of the tumor-bearing Balb/c mice (n=10) per group was compared. While cisplatin single treatment group lost body weight as the days increased due to cytotoxic effects, disulfiram single treatment was relatively healthy as compared to control mice. While the combination group maintained an average weight ranging between the single treatment groups.

2.5. Reduction in tumor volume and immunofluorescence expression *in vivo*.

To confirm the combination effects of disulfiram and cisplatin *in vivo*. The mice were sacrificed short term at 54 days post-injection, and the tumor volume by different drug treatments was pathologically examined. The tumor volume of disulfiram and cisplatin combined group was significantly smaller than that of the control group (Figure 14A). Together these results indicate that the combination group treatment was dramatically more effective as compared to single treatments in reducing tumor volume. The *in vivo* effects of drug combination was also examined by immunofluorescence of AT/RT tumor tissues, ALDH1 expression decreased significantly as compared to control, whereas that of pDNA-PKcs, γH2Ax, ATF3, and cleaved PARP expressions were seen to be significantly increased as compared to control and single treatment groups. (Figure 14B and Figure 15) These results are consistent with that of protein expression data *in vitro*.

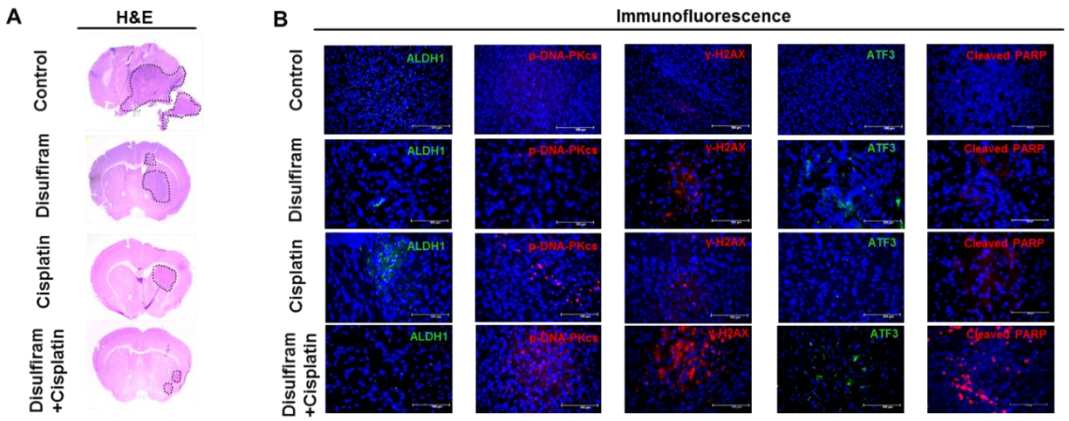

Figure 14: *In vivo* immunofluorescence analysis of drug combination

Mice transplanted with AT/RT cells were grouped into control, disulfiram, cisplatin, and disulfiram+cisplatin. (A) Hematoxylin and eosin (H&E) staining and (B) immunofluorescence against ALDH1, ATF3, p-c-Jun, p-ERK, γ-H2Ax, and cleaved PARP were performed at day 54. Magnification for H&E, x1.25. The outlines indicate tumor margins. Scale bar for immunofluorescence, 100μm. Nuclei were counterstained with 4′, 6′-diamidino-2-phenylindole (blue).

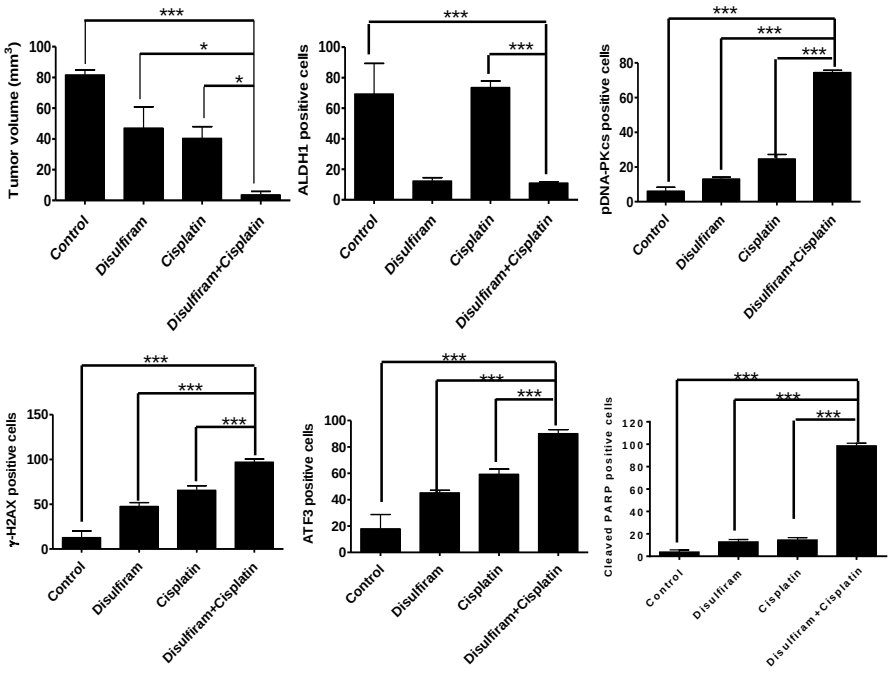

Figure 15: Quantification of tumor volume and immunofluorescence data *in vivo*

The tumor volume and immunofluorescence (IF) data were quantified, by counting the cells expressed by specific antibody via ImageJ software. It was noticed that the tumor volume was reduced when comparing control and single treatment group vs combination group. In case of IF, while ALDH antibody was downregulated in the combination group, it was seen to be synergistically upregulated in pDNA−PKcs, γ−H2Ax, ATF3 and cleaved PARP (*p−0.0373 and ***p−0.0007)

Discussion

Our study demonstrates that the combination of disulfiram and cisplatin synergistically inhibited AT/RT cell viability and enhanced the anti-cancer effect *in vivo*. Importantly, this combination treatment increased cleavage of PARP in AT/RT cells through activation of ATF3.

Atypical teratoid/rhabdoid tumor (AT/RT) is an aggressive tumor of the central nervous system (CNS) that generally includes further treatments post-surgery, which may include radiation, chemotherapy, clinical trials or a combination of treatments (Ginn & Gajjar, 2012). Despite these therapeutic approaches, there is no effective standard treatment for AT/RT. Brain tumor-initiating cells (BTICs), also known as brain cancer stem cells (CSCs) have been proposed as one of the causes of chemoresistance and cancer relapse, as it has the ability to self-renew and to differentiate into the heterogeneous lineages of cancer cells in response to chemotherapeutic agents (Luqmani, 2005; Phi et al., 2018; Reid, Wilson, Li, Marcu, & Bezak, 2017; Trédan, Galmarini, Patel, & Tannock, 2007). In the previous study, ALDH has been described as a stem cell marker in various kinds of tumors including breast (Croker et al., 2009), lung (Ucar et al., 2009) and colorectal cancer (Dalerba et al., 2007), glioblastoma (Rasper et al., 2010) as well as AT/RT (S. A. Choi, Lee, et al., 2014). The proportion of ALDH+ cells was reported to be 23.50% + 5.30% in the serum-free stem cell culture condition (S. A. Choi, Lee, et al., 2014), and in our present study, 2.21 – 5.57% in FBS-containing culture condition. Importantly, the knockdown of ALDH significantly reduces stem capabilities and stem cell-related protein expression.

Disulfiram is an FDA approved ALDH inhibitor that has been used for decades to treat alcoholism by preventing the conversion of acetaldehyde to acetic acid (Sauna, Shukla, & Ambudkar, 2005). Recent studies have shown that disulfiram has an anticancer effect by compromising BTIC function (S. A. Choi, Choi, et al., 2014; P. Liu et al., 2012; Triscott et al., 2012). The combination therapy, using conventional anticancer drugs with BTICs targeting agent, can offer a promising strategy for managing and eradicating different types of cancers (Dragu, Necula, Bleotu, Diaconu, & Chivu-Economescu, 2015; Piccolo, Menale, & Crispi, 2015). In our study, we tested the combination of disulfiram targeting BTICs with three conventional anticancer drugs such as cisplatin, etoposide, and 4HC (4-hydroperoxycyclophosphamide) which is an activated form of cyclophosphamide. We found synergistic effect of AT/RT cell viability in combination of disulfiram with cisplatin. Among the three different drug combinations, cisplatin was found to be the most effective in inhibiting AT/RT cell growth, so further studies were conducted. On the other hand, the effects of disulfiram with etoposide *in vitro* were not significant, and the anticancer effects of disulfiram with 4HC were not observed in AT/RT animal model experiments (S. A. Choi, Choi, et al., 2014).

While cisplatin represented a major landmark in the history of successful anti-cancer drugs, its success and efficacy are waning in the face of therapeutic resistance (Fennell et al., 2016; Gatzemeier et al., 2007; Giaccone et al., 2004; Gore et al., 1989; Siddik, 2003; Wozniak et al., 1998). It has now been well established that ALDH+ cells within the tumors are responsible for resistance to chemotherapeutic agents. ALDH+ CSCs have been consistently shown to exhibit increased chemoresistance, where the extent

of ALDH+ subpopulation often correlates with acquired platinum resistance in ovarian and lung tumors (Duester, 1998; Mizuno et al., 2015). Interestingly, the enzyme activity of ALDH *in vitro* was more reduced in our combination treatment of disulfiram with cisplatin as compared to single treatment. Our study showed that the serial combination of drugs not only reduced the overall IC_{50} drug doses calculated but also significantly inhibits ALDH enzyme activity.

Several other cellular mechanisms of resistance to platinum-based chemotherapeutics are multifactorial and limit its use in clinical practice (St Germain, O'Brien, & Dimitroulakos, 2010). They include molecular events such an inhibiting drug-DNA interaction, and a decrease in induction of apoptosis downstream of the initial reaction of cisplatin (Stewart, 2007). Two significant pathways have been demonstrated to play key roles in this process including mitogen-activated protein kinase (MAPK) cascades (ERK, extracellular signal-regulated kinases; JNK, c-Jun N-terminal kinases; and p38 kinases) and tumor suppressor p53 (Manic et al., 2003; Sedletska, Giraud-Panis, & Malinge, 2005). These kinases along with p53 have been known to be activated following exposure to cisplatin and play a role in regulating cisplatin-induced apoptosis. However, the downstream targets of these pathways have not been well characterized. Employing RNA-seq transcriptome analysis identified a MAPKinase-induced cellular stress pathway, highlighted by activating transcription factor 3 (ATF3) (Cai et al., 2000; Lu, Chen, & Hai, 2007) which is an ATF/ cAMP-responsive element-binding protein (CREB) family member. It is found to be involved in a broad spectrum of cellular stresses, including DNA damage (Y. Liu et al., 2013) , cellular injury (Kaneko, Kiryu-

Seo, Matsumoto, & Kiyama, 2017), oxidative stress and oncogenic stimuli (Wang et al., 2016) and was also shown to regulate diverse cellular functions by either binding to the ATF/CREB cis-regulatory element or interacting with other proteins, such as p53 and NF-κB (Wu et al., 2017). Several reports indicate that ATF3 expression is downregulated in a variety of human cancers, including colon cancer (G. H. Park, Song, & Jeong, 2017), liver cancer (Xiaoyan et al., 2014), multiple myeloma (Ri, 2016), neuroblastoma (Tian et al., 2009), bladder cancer (Yuan et al., 2013), prostate cancer (Wang & Yan, 2016), malignant gliomas (Guenzle et al., 2017) and non-small cell lung carcinoma (Bar et al., 2016). ATF3 may inhibit tumor formation by inducing cell cycle arrest and apoptosis (Wong, 2011). It was also seen to be associated with breast cancer-initiating features such as increased $CD24^{low}$ – $CD44^{high}$ population of cells (Yin et al., 2010). It was seen to be downregulated in glioblastoma stem cells and its expression promotes the transcription of a number of anti-tumorigenic genes (Yan, Yang, & Rich, 2013). Since ATF3 was specifically induced by cisplatin in sensitive but not resistant cells, it is considered to be a key regulator of cisplatin-induced cytotoxicity and resistance. It was also seen to be upregulated when treated with disulfiram (O'Brien et al., 2012). Considering elevated and sustained levels of stress-induced ATF3 enhance apoptosis, ATF3 inducers like disulfiram in combination with cisplatin may enhance the cytotoxic activity of the drug and can represent a novel and rational therapeutic approach.

The amalgamation of anti-cancer drugs enhances the efficacy of the treatment as compared to a single drug therapy approach because it targets the key pathways in a

characteristically synergistic or an additive manner (Ashburn & Thor, 2004; Blagosklonny, 2008; Chong & Sullivan Jr, 2007; Quinn et al., 2015). The combination treatment successfully managed to induce apoptosis within the tumor cells via activation of the cleaved PARP mechanism. In doing so, disulfiram inhibited the expression of ALDH1 enzyme found in the cell cytoplasm and also affecting ATF3 which induces a wide variety of cellular stress agents along with cisplatin (Sauna et al., 2005). Furthermore, disulfiram activated other cell stress proteins like pDNA−PKcs and γ−H2Ax in combination with cisplatin. While cisplatin single treatment affected the MAPK and p53 pathway (Achkar et al., 2018; Bragado, Armesilla, Silva, & Porras, 2007).

It is a well−known fact that cisplatin at high doses causes cytotoxic effects amongst patients. Its use in chemotherapy of resistant cancers is limited due to its dose−dependent nephrotoxicity (Khairnar et al., 2019; Miller, Tadagavadi, Ramesh, & Reeves, 2010). Preclinical studies have revealed that disulfiram and it's copper chelate sensitizes chemotherapy−resistant cancer cells to cisplatin and increases its therapeutic index. Cisplatin causes loss of copper from the kidney tissues and further contributes to nephrotoxicity. Diethyldithiocarbamate (DEDC) which is a metabolite of disulfiram, is known to reduce cisplatin related nephrotoxicity even after single−dose administration. The DEDC effectively controls kidney platinum levels and restricts the loss of copper from the kidney (Borch & Pleasants, 1979). An *in vivo* study also showed that a single dose of 5mg/kg i.p. induced observable alternations like ruptured glomeruli, widening of tubular space and infiltration of inflammatory cells with a significant decrease in body weight, while disulfiram treatment significantly inhibited cisplatin−induced nephrotoxicity (Khairnar et al., 2019). Further protection from lipid

peroxidation based damage, nitric oxide–based inflammatory responses, and antioxidative effects have all seemed to reduce with the addition of disulfiram and decrease further with the help of copper chelates associated with it.

It is important to reduce the dosage of cisplatin due to its dose–dependent toxicity. In our study, cisplatin single treatment induced more side effects and weight loss in the mice. Cisplatin had a reduced overall median survival of 37 days with a drastic drop in body weight while that of disulfiram single treatment had an overall median survival of 69 days as compared to the combination treatment, which not only had a higher median survival of 75 days post–treatment but also managed to maintain optimum body weight *in vivo*.

In light of preclinical evidence that disulfiram and its related metabolic compounds can decrease the toxicity and increase the therapeutic index of cisplatin, various clinical trials both in phase 2 and phase 3 have been conducted by various other research groups. Disulfiram as a single treatment drug has been in used in glioblastoma or in combination with other agents such as copper gluconate and temozolomide along with radiation therapy. Disulfiram is been considered as a reasonably safe drug and hence been used on a daily basis in a dose range of 100–1000 mg depending on different combination compounds in various clinical trials ("Disulfiram and Copper Gluconate With Temozolomide in Unmethylated Glioblastoma Multiforme," ; "Disulfiram in Recurrent Glioblastoma," ; "Disulfiram in Treating Patients With Glioblastoma Multiforme After Radiation Therapy With Temozolomide," ; "Disulfiram/Copper With Concurrent Radiation Therapy and Temozolomide in Patients With Newly Diagnosed Glioblastoma," ;

"Safety, Tolerability and Efficacy of Disulfiram and Copper Gluconate in Recurrent Glioblastoma,"). It was also found to reduce cancer-specific mortality for cancers overall as well as for cancers of the colon, prostate, and breast (Skrott et al., 2017). But the intriguing aspect is that the use of disulfiram as a cancer drug is fairly recent in brain tumors and hence most of these trials are either in recruiting phase or in their final stages of completion.

There have been further studies using both disulfiram and cisplatin combination in other target tumors such as lung cancer, prostate cancer, adenocarcinomas, carcinoma in thyroid and adrenal glands and a current study on germ cell tumors. A Phase I study from 1987 targeted various solid tumors in patients. Herein, cisplatin was administered intravenously to 11 patients and via hepatic artery to one patient at 100 mg/m^2. To determine the dose-limiting toxicity of disulfiram, a dose range of 500 – 3000 mg/m^2 was administered 1 hour before the end of a 2-hour cisplatin infusion. Post-treatment only eight patients were evaluable for response to treatment, two were inevaluable because they died from tumor-related causes and two were inevaluable because they had no evaluable disease at the initiation of treatment. The results include a partial response rate of 25% (two patients with thymoma and adenosquamous carcinoma of the lung). Patient with transitional cell carcinoma of renal pelvis had tumor shrinkage of <50% and was in a stable disease category. The patient with adrenal cortical carcinoma experienced a mixed response, with shrinkage in some pulmonary metastases and growth in others. And three patients with prostate carcinoma and squamous cell carcinoma failed on treatment (Stewart, Verma, & Maroun, 1987). A Phase IIb trial was

also conducted from 2009 to 2015 using disulfiram and cisplatin in metastatic non−small cell lung cancer (NSCLC). Forty newly diagnosed patients were recruited from stage IV cancer. The patients were treated only with chemotherapy and none with surgery or radiation. Disulfiram was administered at 40 mg three times daily along with cisplatin and vinorelbine for six cycles. The patients were treated for more than two cycles half with and half without disulfiram. Results include an increase in survival rate for the experimental group (10 months vs 7.1 months). There were only two long−term survivors and both were from disulfiram treated group. Which is an unusual result in stage IV lung cancer patients treated by chemotherapy alone (Nechushtan et al., 2015). Finally, a current clinical trial which is underway, dealing with refractory testicular germ cell tumors (TGCTs) that has started recruiting patients since May 2019 and will test the response of cisplatin at 50mg/m^2 for first two days and 400mg disulfiram daily for 3 weeks. The results of which are expected to be declared by Dec 2022 ("Disulfiram and Cisplatin in Refractory TGCTs,"). This goes to show that the current use of disulfiram is a "hot topic" in cancers and brain tumors with the combination of disulfiram and cisplatin being researched and gaining some success in other tumors. Also suggesting that combination treatment can be more effective in reducing tumor volume as compared to single treatment, which supports our theory. Furthermore, if positive results are obtained from these trials, it might be possible to implement our drug combination in pediatric tumors, particularly in AT/RT.

In our study, the drug combination of disulfiram and cisplatin provides an effective and safe treatment strategy against AT/RT. Treatment with disulfiram can target the

causative cells at a therapeutic limit followed by cisplatin which has been suggested to be an obstacle due to its dose-dependent toxicity. In combination, disulfiram may offer possibility of increasing the efficacy and reducing the overall drug dose to a safe limit. Our *in vivo* study suggests that the combination of disulfiram and cisplatin effectively reduced tumor volume (sacrificed at 54 days) and increased the overall survival as compared to control and single treatment group. In conclusion, our results elucidate that the combined chemotherapeutic treatment strategy shows an anticancer effect on AT/RT both *in vitro* and *in vivo* by activating the cellular apoptosis mechanism via cleaved PARP. The drugs activated DNA damage proteins like γH2Ax and pDNA-PKcs followed by the upregulation of ATF3 downstream leading to an increased tumor cell death. Considering there is a lack of an adequate chemotherapeutics for AT/RT, the combination of disulfiram and cisplatin may be considered as a viable option for treatment against AT/RT.

References

Achkar, Iman W, Abdulrahman, Nabeel, Al-Sulaiti, Hend, Joseph, Jensa Mariam, Uddin, Shahab, & Mraiche, Fatima. (2018). Cisplatin based therapy: the role of the mitogen activated protein kinase signaling pathway. *Journal of translational medicine, 16*(1), 96.

Al-Lazikani, Bissan, Banerji, Udai, & Workman, Paul. (2012). Combinatorial drug therapy for cancer in the post-genomic era. *Nature biotechnology, 30*(7), 679.

Arruebo, Manuel, Vilaboa, Nuria, Sáez-Gutierrez, Berta, Lambea, Julio, Tres, Alejandro, Valladares, Mónica, & González-Fernández, África. (2011). Assessment of the evolution of cancer treatment therapies. *Cancers, 3*(3), 3279-3330.

Ashburn, Ted T, & Thor, Karl B. (2004). Drug repositioning: identifying and developing new uses for existing drugs. *Nature reviews Drug discovery, 3*(8), 673.

Bar, Jair, Hasim, Mohamed S, Baghai, Tabassom, Niknejad, Nima, Perkins, Theodore J, Stewart, David J, Dimitroulakos, Jim. (2016). Induction of activating transcription factor 3 is associated with cisplatin responsiveness in non-small cell lung carcinoma cells. *Neoplasia, 18*(9), 525-535.

Biswas, Ahitagni, Kashyap, Lakhan, Kakkar, Aanchal, Sarkar, Chitra, & Julka, Pramod Kumar. (2016). Atypical teratoid/rhabdoid tumors: challenges and search for solutions. *Cancer management and research, 8*, 115.

Blagosklonny, Mikhail V. (2008). "Targeting the absence" and therapeutic engineering for cancer therapy. *Cell Cycle, 7*(10), 1307-1312.

Bodenner, Donald L, Dedon, Peter C, Keng, Peter C, Katz, Janet C, & Borch, Richard F. (1986). Selective protection against cis-diamminedichloroplatinum (II)-induced toxicity in kidney, gut, and bone marrow by diethyldithiocarbamate. *Cancer research, 46*(6), 2751-2755.

Borch, Richard F, & Pleasants, Michael E. (1979). Inhibition of cis-platinum nephrotoxicity by diethyldithiocarbamate rescue in a rat model. *Proceedings of the National Academy of Sciences, 76*(12), 6611-6614.

Bragado, Paloma, Armesilla, Alejandro, Silva, Augusto, & Porras, Almudena. (2007). Apoptosis by cisplatin requires p53 mediated p38 α MAPK activation through ROS generation. *Apoptosis, 12*(9), 1733-1742.

Brozovic, Anamaria, & Osmak, Maja. (2007). Activation of mitogen-activated protein kinases by cisplatin and their role in cisplatin-resistance. *Cancer letters, 251*(1), 1-16.

Cai, Yong, Zhang, Chun, Nawa, Tigre, Aso, Teijiro, Tanaka, Makiko, Oshiro, Satoru, Kitajima, Shigetaka. (2000). Homocysteine-responsive ATF3 gene expression in human vascular endothelial cells: activation of c-Jun NH2-terminal kinase and promoter response element. *Blood, 96*(6), 2140-2148.

Chen, Di, Cui, Qiuzhi Cindy, Yang, Huanjie, & Dou, Q Ping. (2006). Disulfiram, a clinically used anti-alcoholism drug and copper-binding agent, induces apoptotic cell death in breast cancer cultures and xenografts via inhibition of the proteasome activity. *Cancer research, 66*(21), 10425-10433.

Chi, Susan N, Zimmerman, Mary Ann, Yao, Xiaopan, Cohen, Kenneth J, Burger, Peter, Biegel, Jaclyn A, Mazewski, Claire. (2009). Intensive multimodality treatment for children with newly diagnosed CNS atypical teratoid rhabdoid tumor. *Journal of Clinical Oncology, 27*(3), 385.

Choi, SA, Lee, YE, Kwak, PA, Lee, JY, Kim, SS, Lee, SJ, Song, SH. (2015). Clinically applicable human adipose tissue-derived mesenchymal stem cells delivering therapeutic genes to brainstem gliomas. *Cancer gene therapy, 22*(6), 302.

Choi, Seung Ah, Choi, Jung Won, Wang, Kyu-Chang, Phi, Ji Hoon, Lee, Ji Yeoun, Park, Kyung Duk, Kim, Seung-Ki. (2014). Disulfiram modulates stemness and metabolism of brain tumor initiating cells in atypical teratoid/rhabdoid tumors. *Neuro-oncology, 17*(6), 810-821.

Choi, Seung Ah, Lee, Ji Yeoun, Phi, Ji Hoon, Wang, Kyu-Chang, Park, Chul-Kee, Park, Sung-Hye, & Kim, Seung-Ki. (2014). Identification of brain tumour initiating cells using the stem cell marker aldehyde dehydrogenase. *European Journal of Cancer, 50*(1), 137-149.

Choi, Seung Ah, Wang, Kyu-Chang, Phi, Ji Hoon, Lee, Ji Yeoun, Park, Chul-Kee, Park, Sung-Hye, & Kim, Seung-Ki. (2012). A distinct subpopulation within

CD133 positive brain tumor cells shares characteristics with endothelial progenitor cells. *Cancer letters, 324*(2), 221-230.

Chong, Curtis R, & Sullivan Jr, David J. (2007). New uses for old drugs. *Nature, 448*(7154), 645.

Croker, Alysha K, Goodale, David, Chu, Jenny, Postenka, Carl, Hedley, Benjamin D, Hess, David A, & Allan, Alison L. (2009). High aldehyde dehydrogenase and expression of cancer stem cell markers selects for breast cancer cells with enhanced malignant and metastatic ability. *Journal of cellular and molecular medicine, 13*(8b), 2236-2252.

Cvek, B. (2011). Targeting malignancies with disulfiram (Antabuse): multidrug resistance, angiogenesis, and proteasome. *Current cancer drug targets, 11*(3), 332-337.

Dalerba, Piero, Dylla, Scott J, Park, In-Kyung, Liu, Rui, Wang, Xinhao, Cho, Robert W, Simeone, Diane M. (2007). Phenotypic characterization of human colorectal cancer stem cells. *Proceedings of the National Academy of Sciences, 104*(24), 10158-10163.

Dirks, Peter B. (2010). Brain tumor stem cells: the cancer stem cell hypothesis writ large. *Molecular oncology, 4*(5), 420-430.

Disulfiram and Cisplatin in Refractory TGCTs.). from https://ClinicalTrials.gov/show/NCT03950830

Disulfiram and Copper Gluconate With Temozolomide in Unmethylated Glioblastoma Multiforme.). from https://ClinicalTrials.gov/show/NCT03363659

Disulfiram in Recurrent Glioblastoma.). from https://ClinicalTrials.gov/show/NCT02678975

Disulfiram in Treating Patients With Glioblastoma Multiforme After Radiation Therapy With Temozolomide.). from https://ClinicalTrials.gov/show/NCT01907165

Disulfiram/Copper With Concurrent Radiation Therapy and Temozolomide in Patients With Newly Diagnosed Glioblastoma.). from https://ClinicalTrials.gov/show/NCT02715609

Dragu, Denisa L, Necula, Laura G, Bleotu, Coralia, Diaconu, Carmen C, & Chivu-Economescu, Mihaela. (2015). Therapies targeting cancer stem cells: Current trends and future challenges. *World journal of stem cells, 7*(9), 1185.

Duester, Gregg. (1998). Alcohol dehydrogenase as a critical mediator of retinoic acid synthesis from vitamin A in the mouse embryo. *The Journal of nutrition, 128*(2), 459S-462S.

Fennell, DA, Summers, Y, Cadranel, J, Benepal, T, Christoph, DC, Lal, R, . . . Ferry, D. (2016). Cisplatin in the modern era: The backbone of first-line chemotherapy for non-small cell lung cancer. *Cancer treatment reviews, 44*, 42-50.

Galanski, Markus. (2006). Recent developments in the field of anticancer platinum complexes. *Recent patents on anti-cancer drug discovery, 1*(2), 285-295.

Gatzemeier, Ulrich, Pluzanska, Anna, Szczesna, Aleksandra, Kaukel, Eckhard, Roubec, Jaromir, De Rosa, Flavio, Serwatowski, Piotr. (2007). Phase III study

of erlotinib in combination with cisplatin and gemcitabine in advanced non-small-cell lung cancer: The Tarceva Lung Cancer Investigation Trial. *Journal of Clinical Oncology, 25*(12), 1545-1552.

Germano, Isabelle, Swiss, Victoria, & Casaccia, Patrizia. (2010). Primary brain tumors, neural stem cell, and brain tumor cancer cells: where is the link? *Neuropharmacology, 58*(6), 903-910.

Gessi, Marco, Giangaspero, Felice, & Pietsch, Torsten. (2003). Atypical teratoid/rhabdoid tumors and choroid plexus tumors: when genetics "surprise" pathology. *Brain pathology, 13*(3), 409-414.

Giaccone, Giuseppe, Herbst, Roy S, Manegold, Christian, Scagliotti, Giorgio, Rosell, Rafael, Miller, Vincent, Pluzanska, Anna. (2004). Gefitinib in combination with gemcitabine and cisplatin in advanced non-small-cell lung cancer: a phase III trial—INTACT 1. *Journal of Clinical Oncology, 22*(5), 777-784.

Ginestier, Christophe, Hur, Min Hee, Charafe-Jauffret, Emmanuelle, Monville, Florence, Dutcher, Julie, Brown, Marty, Liu, Suling. (2007). ALDH1 is a marker of normal and malignant human mammary stem cells and a predictor of poor clinical outcome. *Cell stem cell, 1*(5), 555-567.

Ginn, Kevin F, & Gajjar, Amar. (2012). Atypical teratoid rhabdoid tumor: current therapy and future directions. *Frontiers in oncology, 2*, 114.

Gore, ME, Fryatt, I, Wiltshaw, E, Dawson, T, Robinson, BA, & Calvert, AH. (1989). Cisplatin/carboplatin cross-resistance in ovarian cancer. *British journal of cancer, 60*(5), 767.

Guenzle, Jessica, Wolf, Louisa J, Garrelfs, Nicklas WC, Goeldner, Jonathan M, Osterberg, Nadja, Schindler, Cora R, Weyerbrock, Astrid. (2017). ATF3 reduces migration capacity by regulation of matrix metalloproteinases via NF κ B and STAT3 inhibition in glioblastoma. *Cell death discovery, 3*, 17006.

Hacker, Miles P, Ershler, William B, Newman, Robert A, & Gamelli, Richard L. (1982). Effect of disulfiram (tetraethylthiuram disulfide) and diethyldithiocarbamate on the bladder toxicity and antitumor activity of cyclophosphamide in mice. *Cancer research, 42*(11), 4490-4494.

Han, Zhi-Yan, Richer, Wilfrid, Fréneaux, Paul, Chauvin, Céline, Lucchesi, Carlo, Guillemot, Delphine, Masliah-Planchon, Julien. (2016). The occurrence of intracranial rhabdoid tumours in mice depends on temporal control of Smarcb1 inactivation. *Nature communications, 7*, 10421.

Hanumantha Rao Madala, Surendra R Punganuru, Ali-Osman, Francis, Zhang, Ruiwen, & Srivenugopal, Kalkunte S. (2018). Brain-and brain tumor-penetrating disulfiram nanoparticles: Sequence of cytotoxic events and efficacy in human glioma cell lines and intracranial xenografts. *Oncotarget, 9*(3), 3459.

Hill, JM, & Speer, RJ. (1982). Organo-platinum complexes as antitumor agents. *Anticancer research, 2*(3), 173-186.

Ho, DM-T, Hsu, C-Y, Wong, T-T, Ting, L-T, & Chiang, Hung. (2000). Atypical teratoid/rhabdoid tumor of the central nervous system: a comparative study

with primitive neuroectodermal tumor/medulloblastoma. *Acta neuropathologica, 99*(5), 482-488.

Ho, Lena, & Crabtree, Gerald R. (2010). Chromatin remodelling during development. *Nature, 463*(7280), 474.

Johann, Pascal D, Erkek, Serap, Zapatka, Marc, Kerl, Kornelius, Buchhalter, Ivo, Hovestadt, Volker, Wang, Maia Segura. (2016). Atypical teratoid/rhabdoid tumors are comprised of three epigenetic subgroups with distinct enhancer landscapes. *Cancer cell, 29*(3), 379-393.

Kaneko, Aoi, Kiryu-Seo, Sumiko, Matsumoto, Sakiko, & Kiyama, Hiroshi. (2017). Damage-induced neuronal endopeptidase (DINE) enhances axonal regeneration potential of retinal ganglion cells after optic nerve injury. *Cell death & disease, 8*(6), e2847.

Kelland, Lloyd. (2007). The resurgence of platinum-based cancer chemotherapy. *Nature Reviews Cancer, 7*(8), 573.

Khairnar, Shraddha I, Mahajan, Umesh B, Patil, Kalpesh R, Patel, Harun M, Shinde, Sachin D, Goyal, Sameer N, Patil, Chandragouda R. (2019). Disulfiram and Its Copper Chelate Attenuate Cisplatin-Induced Acute Nephrotoxicity in Rats Via Reduction of Oxidative Stress and Inflammation. *Biological trace element research*, 1-11.

Koppaka, Vindhya, Thompson, David C, Chen, Ying, Ellermann, Manuel, Nicolaou, Kyriacos C, Juvonen, Risto O, Vasiliou, Vasilis. (2012). Aldehyde dehydrogenase inhibitors: a comprehensive review of the pharmacology,

mechanism of action, substrate specificity, and clinical application. *Pharmacological reviews, 64*(3), 520-539.

Lafay-Cousin, L, Hawkins, C, Carret, AS, Johnston, D, Zelcer, S, Wilson, B, Fryer, C. (2012). Central nervous system atypical teratoid rhabdoid tumours: the Canadian Paediatric Brain Tumour Consortium experience. *European journal of cancer, 48*(3), 353-359.

Lee, Young Eun, Choi, Seung Ah, Kwack, Pil Ae, Kim, Hak Jae, Kim, Il Han, Wang, Kyu-Chang, Park, Sung-Hye. (2017). Repositioning disulfiram as a radiosensitizer against atypical teratoid/rhabdoid tumor. *Neuro-oncology, 19*(8), 1079-1087.

Liu, P, Brown, S, Goktug, T, Channathodiyil, P, Kannappan, V, Hugnot, JP, Darling, JL. (2012). Cytotoxic effect of disulfiram/copper on human glioblastoma cell lines and ALDH-positive cancer-stem-like cells. *British journal of cancer, 107*(9), 1488.

Liu, Yongqing, Gao, Fengbin, Jiang, Hanming, Niu, Leilei, Bi, Yiling, Young, Charles YF, Lou, Hongxiang. (2013). Induction of DNA damage and ATF3 by retigeric acid B, a novel topoisomerase II inhibitor, promotes apoptosis in prostate cancer cells. *Cancer letters, 337*(1), 66-76.

Louis, David N, Ohgaki, Hiroko, Wiestler, Otmar D, Cavenee, Webster K, Burger, Peter C, Jouvet, Anne, Kleihues, Paul. (2007). The 2007 WHO classification of tumours of the central nervous system. *Acta neuropathologica, 114*(2), 97-109.

Lu, Dan, Chen, Jingchun, & Hai, Tsonwin. (2007). The regulation of ATF3 gene expression by mitogen-activated protein kinases. *Biochemical Journal, 401*(2), 559-567.

Luqmani, YA. (2005). Mechanisms of drug resistance in cancer chemotherapy. *Medical Principles and Practice, 14*(Suppl. 1), 35-48.

Manic, S, Gatti, L, Carenini, N, Fumagalli, G, Zunino, F, & Perego, P. (2003). Mechanisms controlling sensitivity to platinum complexes: role of p53 and DNA mismatch repair. *Current cancer drug targets, 3*(1), 21-29.

Marcato, Paola, Dean, Cheryl A, Pan, Da, Araslanova, Rakhna, Gillis, Megan, Joshi, Madalsa, Gujar, Shashi. (2011). Aldehyde dehydrogenase activity of breast cancer stem cells is primarily due to isoform ALDH1A3 and its expression is predictive of metastasis. *Stem cells, 29*(1), 32-45.

Miller, Ronald P, Tadagavadi, Raghu K, Ramesh, Ganesan, & Reeves, William Brian. (2010). Mechanisms of cisplatin nephrotoxicity. *Toxins, 2*(11), 2490-2518.

Mizuno, Tomoko, Suzuki, Noriko, Makino, H, Furui, T, Morii, E, Aoki, H, Hirashima, Y. (2015). Cancer stem-like cells of ovarian clear cell carcinoma are enriched in the ALDH-high population associated with an accelerated scavenging system in reactive oxygen species. *Gynecologic oncology, 137*(2), 299-305.

Morgenstern, Daniel A, Gibson, Sian, Brown, Tanya, Sebire, Neil J, & Anderson, John. (2010). Clinical and pathological features of paediatric malignant rhabdoid tumours. *Pediatric blood & cancer, 54*(1), 29-34.

Mutschler, J, Grosshans, M, Soyka, M, & Rösner, S. (2016). Current findings and mechanisms of action of disulfiram in the treatment of alcohol dependence. *Pharmacopsychiatry, 49*(04), 137-141.

Nechushtan, Hovav, Hamamreh, Yousef, Nidal, Salim, Gotfried, Maya, Baron, Amichai, Shalev, Yossi Israeli, Peylan-Ramu, Nili. (2015). A phase IIb trial assessing the addition of disulfiram to chemotherapy for the treatment of metastatic non-small cell lung cancer. *The oncologist, 20*(4), 366-367.

Neuwelt, Alexander J, Nguyen, Tam, Wu, Y Jeffrey, Donson, Andrew M, Vibhakar, Rajeev, Venkatamaran, Sujatha, Foreman, Nicholas K. (2014). Preclinical high-dose acetaminophen with N-acetylcysteine rescue enhances the efficacy of cisplatin chemotherapy in atypical teratoid rhabdoid tumors. *Pediatric blood & cancer, 61*(1), 120-127.

O'Brien, Anna, Barber, Janet EB, Reid, Stephanie, Niknejad, Nima, & Dimitroulakos, Jim. (2012). Enhancement of cisplatin cytotoxicity by disulfiram involves activating transcription factor 3. *Anticancer research, 32*(7), 2679-2688.

Oun, Rabbab, Moussa, Yvonne E, & Wheate, Nial J. (2018). The side effects of platinum-based chemotherapy drugs: a review for chemists. *Dalton transactions, 47*(19), 6645-6653.

Papaioannou, Margarita, Mylonas, Ioannis, Kast, Richard E, & Brüning, Ansgar. (2014). Disulfiram/copper causes redox-related proteotoxicity and concomitant heat shock response in ovarian cancer cells that is augmented by auranofin-mediated thioredoxin inhibition. *Oncoscience, 1*(1), 21.

Park, Gwang Hun, Song, Hun Min, & Jeong, Jin Boo. (2017). Kahweol from coffee induces apoptosis by Upregulating activating transcription factor 3 in human colorectal Cancer cells. *Biomolecules & therapeutics, 25*(3), 337.

Park, Young Min, Go, Yoon Young, Shin, Sun Hwa, Cho, Jae-Gu, Woo, Jeong-Soo, & Song, Jae-Jun. (2018). Anti-cancer effects of disulfiram in head and neck squamous cell carcinoma via autophagic cell death. *PloS one, 13*(9), e0203069.

Parker, Jonathon J, Canoll, Peter, Niswander, Lee, Kleinschmidt-DeMasters, BK, Foshay, Kara, & Waziri, Allen. (2018). Intratumoral heterogeneity of endogenous tumor cell invasive behavior in human glioblastoma. *Scientific reports, 8*(1), 18002.

Pawel, Bruce R. (2018). SMARCB1-deficient tumors of childhood: a practical guide. *Pediatric and Developmental Pathology, 21*(1), 6-28.

Phi, Lan Thi Hanh, Sari, Ita Novita, Yang, Ying-Gui, Lee, Sang-Hyun, Jun, Nayoung, Kim, Kwang Seock, Kwon, Hyog Young. (2018). Cancer stem cells (CSCs) in drug resistance and their therapeutic implications in cancer treatment. *Stem cells international, 2018*.

Piccolo, Maria Teresa, Menale, Ciro, & Crispi, Stefania. (2015). Combined anticancer therapies: an overview of the latest applications. *Anti-cancer agents in medicinal chemistry, 15*(4), 408-422.

Quinn, Bridget A, Dash, Rupesh, Sarkar, Siddik, Azab, Belal, Bhoopathi, Praveen, Das, Swadesh K, Sarkar, Devanand. (2015). Pancreatic cancer combination

therapy using a BH3 mimetic and a synthetic tetracycline. *Cancer research, 75*(11), 2305-2315.

Rasper, Michael, Schäfer, Andrea, Piontek, Guido, Teufel, Julian, Brockhoff, Gero, Ringel, Florian, Schlegel, Jürgen. (2010). Aldehyde dehydrogenase 1 positive glioblastoma cells show brain tumor stem cell capacity. *Neuro-oncology, 12*(10), 1024-1033.

Reid, Paul Ambrose, Wilson, Puthenparampil, Li, Yanrui, Marcu, Loredana Gabriela, & Bezak, Eva. (2017). Current understanding of cancer stem cells: Review of their radiobiology and role in head and neck cancers. *Head & neck, 39*(9), 1920-1932.

Ri, Masaki. (2016). Endoplasmic-reticulum stress pathway-associated mechanisms of action of proteasome inhibitors in multiple myeloma. *International journal of hematology, 104*(3), 273-280.

Richardson, Elizabeth Anne, Ho, Ben, & Huang, Annie. (2018). Atypical teratoid rhabdoid tumour: from tumours to therapies. *Journal of Korean Neurosurgical Society, 61*(3), 302.

Safety, Tolerability and Efficacy of Disulfiram and Copper Gluconate in Recurrent Glioblastoma.). from https://ClinicalTrials.gov/show/NCT03034135

Sauna, Zuben E, Shukla, Suneet, & Ambudkar, Suresh V. (2005). Disulfiram, an old drug with new potential therapeutic uses for human cancers and fungal infections. *Molecular BioSystems, 1*(2), 127-134.

Sawyers, Charles. (2004). Targeted cancer therapy. *Nature, 432*(7015), 294.

Schatton, Tobias, Frank, Natasha Y, & Frank, Markus H. (2009). Identification and targeting of cancer stem cells. *Bioessays, 31*(10), 1038-1049.

Sedletska, Yuliya, Giraud-Panis, Marie-Josèphe, & Malinge, Jean-Marc. (2005). Cisplatin is a DNA-damaging antitumour compound triggering multifactorial biochemical responses in cancer cells: importance of apoptotic pathways. *Current Medicinal Chemistry-Anti-Cancer Agents, 5*(3), 251-265.

Shewach, Donna S, & Kuchta, Robert D. (2009). Introduction to cancer chemotherapeutics: ACS Publications.

Siddik, Zahid H. (2003). Cisplatin: mode of cytotoxic action and molecular basis of resistance. *Oncogene, 22*(47), 7265.

Skrott, Zdenek, Mistrik, Martin, Andersen, Klaus Kaae, Friis, Søren, Majera, Dusana, Gursky, Jan, Moudry, Pavel. (2017). Alcohol-abuse drug disulfiram targets cancer via p97 segregase adaptor NPL4. *Nature, 552*(7684), 194.

Slavc, Irene, Chocholous, Monika, Leiss, Ulrike, Haberler, Christine, Peyrl, Andreas, Azizi, Amedeo A, Widhalm, Georg. (2014). Atypical teratoid rhabdoid tumor: improved long-term survival with an intensive multimodal therapy and delayed radiotherapy. The Medical University of Vienna Experience 1992–2012. *Cancer medicine, 3*(1), 91-100.

St Germain, Carly, O'Brien, Anna, & Dimitroulakos, Jim. (2010). Activating Transcription Factor 3 regulates in part the enhanced tumour cell cytotoxicity of the histone deacetylase inhibitor M344 and cisplatin in combination. *Cancer cell international, 10*(1), 32.

Stewart, David J. (2007). Mechanisms of resistance to cisplatin and carboplatin. *Critical reviews in oncology/hematology, 63*(1), 12-31.

Stewart, David J, Verma, Shailendra, & Maroun, Jean A. (1987). Phase I study of the combination of disulfiram with cisplatin. *American journal of clinical oncology, 10*(6), 517-519.

Sung, Ki Woong, Yoo, Keon Hee, Cho, Eun Joo, Koo, Hong Hoe, Lim, Do Hoon, Shin, Hyung Jin, Ghim, Thad T. (2007). High-dose chemotherapy and autologous stem cell rescue in children with newly diagnosed high-risk or relapsed medulloblastoma or supratentorial primitive neuroectodermal tumor. *Pediatric blood & cancer, 48*(4), 408-415.

Swartling, Fredrik J, Čančer, Matko, Frantz, Aaron, Weishaupt, Holger, & Persson, Anders I. (2015). Deregulated proliferation and differentiation in brain tumors. *Cell and tissue research, 359*(1), 225-254.

Tang, Liling, Nogales, Eva, & Ciferri, Claudio. (2010). Structure and function of SWI/SNF chromatin remodeling complexes and mechanistic implications for transcription. *Progress in biophysics and molecular biology, 102*(2-3), 122-128.

Tian, Ze, An, Ning, Zhou, Bin, Xiao, Peigen, Kohane, Isaac S, & Wu, Erxi. (2009). Cytotoxic diarylheptanoid induces cell cycle arrest and apoptosis via increasing ATF3 and stabilizing p53 in SH-SY5Y cells. *Cancer chemotherapy and pharmacology, 63*(6), 1131-1139.

Trédan, Olivier, Galmarini, Carlos M, Patel, Krupa, & Tannock, Ian F. (2007). Drug resistance and the solid tumor microenvironment. *Journal of the National Cancer Institute, 99*(19), 1441-1454.

Triscott, Joanna, Lee, Cathy, Hu, Kaiji, Fotovati, Abbas, Berns, Rachel, Pambid, Mary, Toyota, Eric. (2012). Disulfiram, a drug widely used to control alcoholism, suppresses self-renewal of glioblastoma and overrides resistance to temozolomide. *Oncotarget, 3*(10), 1112.

Ucar, Deniz, Cogle, Christopher R, Zucali, James R, Ostmark, Blanca, Scott, Edward W, Zori, Robert, Moreb, Jan S. (2009). Aldehyde dehydrogenase activity as a functional marker for lung cancer. *Chemico-biological interactions, 178*(1-3), 48-55.

Wang, Ziyan, Kim, Jaejik, Teng, Yong, Ding, Han-Fei, Zhang, Junran, Hai, Tsonwin, Yan, Chunhong. (2016). Loss of ATF3 promotes hormone-induced prostate carcinogenesis and the emergence of CK5+ CK8+ epithelial cells. *Oncogene, 35*(27), 3555.

Wang, Ziyan, & Yan, Chunhong. (2016). Emerging roles of ATF3 in the suppression of prostate cancer. *Molecular & cellular oncology, 3*(1), e1010948.

Wong, Rebecca SY. (2011). Apoptosis in cancer: from pathogenesis to treatment. *Journal of Experimental & Clinical Cancer Research, 30*(1), 87.

Wozniak, Antoinette J, Crowley, John J, Balcerzak, Stanley P, Weiss, Geoffrey R, Spiridonidis, C Harris, Baker, Laurence H, Gandara, David R. (1998). Randomized trial comparing cisplatin with cisplatin plus vinorelbine in the

treatment of advanced non-small-cell lung cancer: a Southwest Oncology Group study. *Journal of Clinical Oncology, 16*(7), 2459-2465.

Wu, Yan-ping, Cao, Chao, Wu, Yin-fang, Li, Miao, Lai, Tian-wen, Zhu, Chen, Shen, Hua-hao. (2017). Activating transcription factor 3 represses cigarette smoke-induced IL6 and IL8 expression via suppressing NF-κB activation. *Toxicology letters, 270*, 17-24.

Xiaoyan, Li, Shengbing, Zang, Yu, Zhang, Lin, Zheng, Chengjie, Lin, Jingfeng, Liu, & Aimin, Huang. (2014). Low expression of activating transcription factor 3 in human hepatocellular carcinoma and its clinicopathological significance. *Pathology-Research and Practice, 210*(8), 477-481.

Yakisich, J Sebastian, Sidén, Åke, Eneroth, Peter, & Cruz, Mabel. (2001). Disulfiram is a potent in vitro inhibitor of DNA topoisomerases. *Biochemical and biophysical research communications, 289*(2), 586-590.

Yan, Kenneth, Yang, Kailin, & Rich, Jeremy Naftali. (2013). The evolving landscape of brain tumor cancer stem cells. *Current opinion in neurology, 26*(6), 701.

Yeh, Pei Yen, Chuang, Shuang-En, Yeh, Kun-Huei, Song, Ying Chyi, Ea, Chee-Kwee, & Cheng, Ann-Lii. (2002). Increase of the resistance of human cervical carcinoma cells to cisplatin by inhibition of the MEK to ERK signaling pathway partly via enhancement of anticancer drug-induced NF κB activation. *Biochemical pharmacology, 63*(8), 1423-1430.

Yin, Xin, Wolford, Christopher C, Chang, Yi-Seok, McConoughey, Stephen J, Ramsey, Stephen A, Aderem, Alan, & Hai, Tsonwin. (2010). ATF3, an

adaptive-response gene, enhances TGF β signaling and cancer-initiating cell features in breast cancer cells. *J Cell Sci, 123*(20), 3558-3565.

Yip, NC, Fombon, IS, Liu, P, Brown, S, Kannappan, V, Armesilla, AL, Wang, W. (2011). Disulfiram modulated ROS-MAPK and NF κ B pathways and targeted breast cancer cells with cancer stem cell-like properties. *British journal of cancer, 104*(10), 1564.

Yoshida, Akira, Hsu, Lily C, & Davé, Vibha. (1992). Retinal oxidation activity and biological role of human cytosolic aldehyde dehydrogenase. *Enzyme, 46*, 239-244.

Yuan, Xiangliang, Yu, Liang, Li, Junhua, Xie, Guohua, Rong, Tingting, Zhang, Liang, . . . Wang, Die. (2013). ATF3 suppresses metastasis of bladder cancer by regulating gelsolin-mediated remodeling of the actin cytoskeleton. *Cancer research, 73*(12), 3625-3637.

Zha, Jie, Chen, Feili, Dong, Huijuan, Shi, Pengcheng, Yao, Yao, Zhang, Yanyan, Wang, Weiguang. (2014). Disulfiram targeting lymphoid malignant cell lines via ROS-JNK activation as well as Nrf2 and NF-kB pathway inhibition. *Journal of translational medicine, 12*(1), 163.

Zimmermann, Arthur, & Zimmermann, Arthur. (2016). Malignant Rhabdoid Tumors and Tumors with Rhabdoid Features. *Tumors and Tumor-Like Lesions of the Hepatobiliary Tract*, 1-25.

국문초록

소아 악성 뇌종양 비정형・유기형간상종양에서 다이설피람과 시스플라틴 병용투여의 시너지 효과

비정형・유기형간상종양 (Atypical teratoid/rhabdoid tumor, AT/RT) 은 일반적으로 3 세 미만의 어린이에게 생기는 악성 종양으로 효과적인 치료법이 없는 실정이다. AT/RT 에 대한 기존의 항암요법들은 독성 때문에 고농도로 처리가 어렵고 이런 항암요법에 반응하지 않거나 저항성을 가지고 있는 암줄기세포들로 인해 치료의 한계에 봉착해 있다. 우리는 이전 연구에서 AT/RT 세포에서 암줄기세포 표지자로 알려져 있는 알데하이드탈수소효소 (Aldehyde dehydrogenase, ALDH)의 활성도가 높은 세포들이 존재하는 것을 확인하였고 ALDH 억제제인 다이설피람을 이용한 치료법에 대한 연구를 진행해왔다. 본 연구에서는 AT/RT 치료법의 향상을 위해 암줄기세포를 표적화 할 수 있는다이설피람 와 기존의 항암제 cisplatin 의 병용투여에 대한 효과 및 그 기전을 밝히고자 하였다.

우리는 2 종류의 AT/RT 환자 유래 1 차 배양 세포와 2 종류의 확립된 세포주를 사용하여 다이설피람와 cisplatin 의 병용 처리하여 세포 생존율 분석, ALDH enzyme activity 측정, 단백질 발현, 면역 형광 시험을 통해 *in vitro* 시험을 수행하였고 AT/RT 동물 모델을 이용하여 *in vivo* live imaging 을 실시하고 종양의 크기 및 장기 생존율에 대해 분석하였다.

그 결과 다이설피람 와 cisplatin 을 병용 처리하게 되면 시너지 항암 효과가 나타나는 것이 관찰되었다. 다이설피람 와 cisplatin 병용 처리는 C-Jun 과 ATF3 단백질 발현을 조절하여 PARP 를 활성화시켜 세포 사멸을 훨씬 더 효과적으로 유발시킬 수 있다는 것을 입증하였다. 뿐만 아니라 AT/RT 동물모델에 병용투여시 종양 크기는 감소시키고 장기생존율을 증가시키는 것을 확인할 수 있었다.

결론적으로, 본 연구는 다이설피람 와 cisplatin 의 병용치료 요법은 기존의 화학요법으로는 치료가 어려운 AT/RT 에 대한 새로운 치료 전략으로 사용될 수 있음을 제시한다.